# Resonances in electron scattering by atoms and ions

V. I. Lend'el, V. T. Navrotskiĭ, and E. P. Sabad

*Uzhgorod State University; Uzhgorod Branch, Institute of Nuclear Research, Academy of Sciences of the Ukrainian SSR*

Usp. Fiz. Nauk **151**, 425–468 (March 1987)

The present state of research on the resonant scattering of electrons by atoms and ions is described. A comparison is made of the various theoretical methods used to describe these processes: the method of strong coupling of channels, the diagonalization method, the $R$-matrix method, etc. For the most part, the latest experimental data over the past five years (through the end of 1984) are reported. Only isolated references are made to 1985 studies. The thrust of the review is to determine the role played by autoionizing states in resonant scattering and to analyze how well the existing theoretical studies describe the experimental data available. It can be concluded from this analysis that we have a fairly clear picture of the mechanism for resonant scattering processes and that the description is qualitatively good. However, an important role is played here by electron-electron correlations. Further research is required for an accurate account of these correlations.

**TABLE OF CONTENTS**



## 1. INTRODUCTION

The scattering of electrons by atoms and ions has recently been attracting increasing interest. The reason is that data on the elementary processes involved in the collisions of electrons with atoms and ions are important for the successful development of such directions in modern physics and new technology as plasma physics, laser technology, fusion power, quantum chemistry, astrophysics, the physics of the upper atmosphere, and the physics of nuclear reactions involving heavy ions. One method for pumping a gas laser, for example, is to use electron impact to excite atoms and ions. In all these processes, an important role is played by quasistationary states of the system consisting of the target and the impinging electron; the decay of these states leads to a complex resonance structure in the scattering cross sections. As it turns out, there is a striking similarity between these resonances and the resonances discovered a long time ago in the scattering of nucleons by nuclei which go through a compound state. Furthermore, resonances of this type have been discovered in the scattering of "elementary" particles by each other (e.g., $\pi N$ scattering) and in fact provide evidence that these particles have a complex (quark) structure.

Back at the Third International Conference on Electron-Atom Collisions in 1963, H. S. W. Massey ranked the discovery of these resonances among the most exciting accomplishments in atomic physics over the past twenty years. Since that time, theoretical and experimental studies of resonances have remained an important field in modern atomic physics.

The first indications of the existence of quasistationary states of atomic systems were obtained by J. Franck and colleagues as far back as 1921, in a study of certain aspects of discharges in neon. In offering an explanation of these aspects, Franck suggested that when an outer-shell electron of a neon atom is excited into a vacant orbital the impinging electron may be captured, and an excited negative neon ion may form.

After a time, similar events were discovered in other atoms also. However, because of the difficulties in producing sufficiently intense sources of monoenergetic electrons and the lack of any applications-driven interest, these studies were not pursued further. Extensive, systematic experimental studies of resonances were resumed only in the early 1960s, since by that time electron beams with a sufficiently small energy spread and a fairly high current ($\sim 10^{-7}$ A) had been developed.

The revival of widespread interest in resonances in atomic systems contributed to the appearance of a pioneering theoretical paper by U. Fano,[1] in which it was shown that the interference of a discrete quasistationary state with the adjacent continuum gives rise to resonances in the cross sec-

 0038-5670/87/030220-26$01.80  

tions for elastic scattering and excitation. Boiling down the theoretical results to specific numbers required extensive computations, which became possible only with the help of modern high-speed computers. Methods were developed which, even before the appearance of experimental studies, made it possible to calculate resonance effects in the scattering of electrons by the hydrogen atom. For example, Burke and Shey[2] discovered a resonance in the elastic scattering of an electron by hydrogen below the excitation threshold. Gailitis and Damburg[3] proposed an explanation for the mechanism for the appearance of these resonances.

The first resonance which was discovered experimentally was the $^2S$ resonance which Schulz observed[4] in elastic e + He scattering. It lies about 0.5 eV below the threshold for 2 $^3S$ He.

Later on, in connection with the significantly increasing interest in research on the resonance structure of cross sections, resonances were found in the scattering of electrons by atoms and ions of inert gases,[5,6] alkali metals,[7-9] alkaline earths,[10,11] mercury atoms,[12] and also molecules.[13]

Studies of resonance phenomena in scattering have been the topics of many excellent reviews (e.g., Refs. 14–20). In the past few years, however, many new experimental and theoretical studies of resonances have been carried out. It is thus clearly worthwhile to examine the present state of this question.

We consider the collision of an electron with some composite target, which may be an atom or ion. We will restrict the discussion below to that region of electron energies in which only a limited number of low-lying excited states of the target, A, can be excited. It turns out that at certain energies of the impinging electron there can be an excitation of the target accompanied by a simultaneous capture of the electron, with the result that a short-lived quasibound state of the e + A system forms. If A is a singly charged positive ion, these states are excited states of a neutral atom in the continuum region. They are called "resonance" or "autoionizing" states, since they may spontaneously decay into an electron and an ion in the ground state or an excited state. If the target is instead a neutral atom, the states which form are the states of a negative ion, which can also decay into an electron and an atom in the ground or in an excited state. In the literature, states of this sort are usually called "self-detaching" states. Nevertheless, again in this case the term "autoionizing" state is sometimes used. To simplify the terminology, we will also use that term here. Generally speaking, autoionizing states can also decay by a radiative mechanism, in which case the decay products are a photon and an atom (or ion) in the ground state or an excited state. Below, however, we will restrict the discussion to processes which involve those autoionizing states whose radiative decay can be ignored. We thus have two possibilities in the scattering of an impinging electron at a certain energy:

$$e + A \begin{cases} \longrightarrow e + A, \\ \longrightarrow A^* \rightarrow e + A, \end{cases}$$

where A is the target in the ground or excited state, and A* is the system in the autoionizing state. These two possibilities interfere, with the result that the cross section acquires a complex resonance structure. Below we will refer to the first of these possibilities as "direct scattering" or "scattering through an open channel," while the second possibility is "scattering through a closed channel."

Since autoionizing states are unstable, they are characterized by a certain width $\Gamma$. On the one hand, this width indicates the uncertainty in the energy of these states, while on the other it represents the probability that the state will decay in a unit time (we are using the atomic system of units).

We will restrict the discussion to low-energy autoionizing states, which form through the excitation of an electron exclusively from the outer shell of the target, with a subsequent capture of the impinging electron. Accordingly, we will, for example, ignore those resonances due to autoionizing states which arise through the formation of vacancies in inner shells of an atom or which stem from the excitation of several electrons from the outer shell.

The goal of the theoretical and experimental research on resonances in scattering is to determine the parameters (energies and widths) of the autoionizing states and their effects on the cross sections for scattering processes. Research is being carried out on the cross sections for both elastic and inelastic scattering (the latter cross sections are also called "excitation cross sections").

Studies of these questions are of both fundamental and applied value. They can reveal subtle details of the mechanism by which electrons interact with atoms and ions. In particular, it turns out that electron-electron correlations play an important role here. In several cases, resonance phenomena are dominant in scattering processes. They also play a role in related processes: photoexcitation, multiphoton ionization, etc.

## 2. THEORY

When an electron collides with an atom, the possibility of elastic scattering is accompanied by the possibility that the atom may undergo simultaneous excitation and ionization, depending on the energy of the electron. Those processes which are allowed at the given energy of the electron determine open channels. The processes which are forbidden from the energy standpoint, in contrast, determine closed channels. It is with the closed channels that we associate resonances in the scattering cross sections which have come to be known as "Feshbach resonances" or "closed-channel resonances." The mechanism for their appearance is the capture by the target of the impinging electron in an autoionizing state through one of the closed channels. The electron, however, may be captured temporarily by the target in an open channel also. A necessary condition for this event is the presence in a certain open channel of a potential of a specific shape: a barrier with a well in which a quasibound state can exist. The capture of an electron by the target, followed by the decay of the quasibound state which has formed, leads in this case to a so-called shape resonance. In contrast with Feshbach resonances, which lie below the target excitation thresholds, shape resonances occur at energies only slightly ($\sim$0.1 eV) above the threshold for the process in whose cross section they appear.

The autoionizing states which are formed during electron capture decay in a time $\tau \sim 1/\Gamma$ into an atom and an electron in the continuous spectrum. The most probable channel for the decay of an autoionizing state is the decay

into the next-lowest state of the atom along the energy scale (provided that this decay is not forbidden by conservation laws). The widths of shape resonances are significantly greater than those of Feshbach resonances, since the energy interval between an autoionizing state and the energy of the atom in the final state is much smaller in the case of shape resonances than in the case of Feshbach resonances.

Let us examine the mechanism for the appearance of closed-channel resonances. For this purpose we will utilize the projection-operator formalism proposed by Feshbach. The problem of the scattering of an electron by an $N$-electron atomic target is reduced to that of solving the Schrödinger equation

$$(H - E)\,\Psi = 0 \tag{1.1}$$

with appropriate boundary conditions. Here $H$ is the Hamiltonian of the system consisting of the target and the electron, and $\Psi$ is the wave function of the system. We denote by $\{\varphi_\nu\}$ the complete system of wave functions of the target (the atom or ion) in the ground and excited states. The wave function ($\Psi$) of the system consisting of the target and the electron can then be written as the expansion

$$\Psi = \sum_\nu A\,[\varphi_\nu F_\nu], \tag{1.2}$$

where the sum over $\gamma$ also implies an integration over the continuum. The functions $F_\gamma$ describe the motion of the external (scattered) electron, and $A$ is an antisymmetrization operator. The sum over $\gamma$ contains both a finite number of terms describing open channels and an infinite number of terms corresponding to closed channels. If $\gamma$ corresponds to an open channel, then the function $F_\gamma$ at infinity contains a diverging wave; otherwise, $F_\gamma$ is quadratically integrable.

We introduce the operator $Q$, which projects onto a subspace of states which are orthogonal to the states $A\,[\varphi_\gamma \overline{F}_\gamma]$, where $\gamma$ corresponds to open channels, and $\overline{F}_\gamma$ is an arbitrary function which has an asymptotic behavior of the same form as that of the function $F_\gamma$. The operator $P = 1 - Q$ then projects onto the subspace of states of open channels. Since we have $P^2 = P$, $Q^2 = Q$, $PQ = QP = 0$, $P + Q = 1$, Schrödinger equation (1.1) can be rewritten as

$$P\,(H - E)\,(P + Q)\,\Psi = 0, \tag{1.3}$$

$$Q\,(H - E)\,(P + Q)\,\Psi = 0. \tag{1.4}$$

Eliminating $Q\Psi$ from Eqs. (1.3), (1.4), we find the equation

$$[P\,(H - E) + W]\,P\Psi = 0, \tag{1.5}$$

where

$$W = PHQ\,[Q\,(E - H)Q^{-1}]QHP. \tag{1.6}$$

the operator $W$ is a nonlocal complex potential which depends on the energy $E$. The potential $W$ is called the "optical potential" (or, on occasion, the "polarization potential"). It describes the effect of all the closed channels. It is this potential which leads, under certain conditions, to the existence of Feshbach resonances. A condition for their appearance is the existence of a discrete spectrum of states $\Phi_n$ of the operator $QHQ$ (Ref. 21):

$$QHQ\Phi_\mu = \varepsilon_\mu \Phi_\mu.$$

If the energy $E$ is close to one of the eigenvalues $\varepsilon_\mu$, a bound state can form in the optical potential and give rise to a resonance in the cross sections.

Since Eq. (1.1) cannot be solved exactly, we cannot find an explicit expression for the optical potential $W$. The various methods for calculating resonances in the cross sections correspond to the replacement of the optical potential by various approximate expressions. Let us examine some of these methods.

### 2.1. Strong-coupling method

One of the most popular approximate methods for solving Eq. (1.1) is the strong-coupling method, whose popularity can be credited to studies by Burke and Seaton,[14,15,22] Damburg and Gaĭlitis,[23] *et al.* We will not discuss this method in detail here; we instead refer the interested reader to the review by Gaĭlitis.[21]

In the strong-coupling method, an approximate solution of Eq. (1.1) is sought in the form of expansion (1.2), which includes all the terms corresponding to open channels but only a finite number of terms describing closed channels. For practical calculations, it is necessary to switch to the total angular momentum representation in expansion (1.2) and to distinguish the radial parts of the function $F_\gamma$. In the $LS$-coupling scheme, the state of the system is characterized by the set of quantum numbers $\Gamma = QlLSM_L M_S$, where $Q = \alpha L_T S_T$ is the set of quantum numbers of the target ($L_T$ and $S_T$ are the orbital angular momentum and the spin of the target), and $L, S, M_L$ and $M_S$ are the total angular momenta of the system and their projections onto the $Z$ axis. We denote by $\Psi(\Gamma\mathbf{X}, \mathbf{X}_{N+1})$ the solution of Eq. (1.1) under the condition that the initial state of the system is characterized by quantum numbers $\Gamma$. Here $\mathbf{X} = (\mathbf{x}_1, \ldots, \mathbf{x}_N)$, $\mathbf{x}_i = (\mathbf{r}_i, \sigma_i)$ is the set of spatial coordinates $\mathbf{r}_i$ and spin coordinates $\sigma_i$ of the $i$th electron. Expansion (1.2) is then written in the form

$$\Psi(\Gamma\mathbf{X},\ \mathbf{x}_{N+1}) = (N+1)^{-1/2} \sum_{p=1}^{N+1} (-1)^{N+1-p} \times \sum_{\Gamma'}^{N} \Psi(\Gamma'\mathbf{X}\hat{r}_p\sigma_p)\,\frac{F_{\Gamma\Gamma'}(r_p)}{r_p}, \tag{1.7}$$

where $N$ is the number of channels.

The function $\Psi'(\Gamma'\mathbf{X}\hat{r}_p\sigma_p)$ incorporates not only the wave function of the target but also the spin-orbit part of the wave function of the external electron.

Using a variational principle, consisting of the requirement that the functional $\langle\Psi|H - E|\Psi\rangle$ be stationary upon a variation of the functions $F_{\Gamma\Gamma'}$ with a certain restriction on the asymptotic behavior of these functions, we can derive[24] a system of integrodifferential equations for the radial functions $F_{\Gamma\Gamma'}$. Solving this system of equations numerically, we then find the radial functions and the scattering matrix.

The accuracy of calculations in the strong-coupling model improves with increasing number of closed channels incorporated in the analysis. As the number of channels considered is increased, however, the number of equations for the radial functions increases. The extent to which this number can increase is obviously limited by the capabilities of the computers. Consequently, accurate results are obtained only at low energies, where the number of open channels is small. Furthermore, the strong-coupling method leads to reliable

results only if it is possible to restrict the study to a small number of closed channels. This is the case when the polarizability of the atom results primarily from a few virtual transitions. In most cases, in contrast, many intermediate states contribute to the polarization. It is difficult to apply the method of strong coupling to such atoms because of the poor convergence of expansion (1.2).

In this case the accuracy of the calculations can sometimes be improved without a great increase in the volume of computations by adding to expansion (1.2) a certain number of "pseudostates" $\bar{\varphi}_\gamma$. To some extent, the pseudostates are called upon to incorporate closed channels which are not incorporated in expansion (1.2). The functions $\bar{\varphi}_\gamma$ are chosen in such a way that the family of states $\varphi_\gamma$ and pseudostates $\bar{\varphi}_\gamma$ which are taken into account leads to the experimentally observed value of the polarizability of the atom. On the other hand, this approach has the disadvantage that the introduction of pseudostates sometimes gives rise to false resonances.

Another way to improve the accuracy of calculations is to add "correlation terms" $\chi_\mu$ to expansion (1.2). The correlation terms are given functions of the bound-state type:

$$\Psi = \sum_\gamma A\,[\varphi_\gamma F_\gamma] + \sum_\mu C_\mu \chi_\mu. \tag{1.8}$$

In this case the Schrödinger equation leads to a system of coupled integrodifferential equations for the radial functions $F_{\Gamma\Gamma'}$ and algebraic equations for the coefficients $C_\mu$. The strong-coupling method modified in this fashion is called the "strong-coupling method with correlation functions."

Many calculations on the scattering of electrons by atoms and ions have been carried out by the strong-coupling method and by the method of strong coupling with correlation functions. We will examine the results of these calculations below. These calculations, however, are exceedingly complicated and tedious and require much time on powerful computers.

At least three circumstances contribute to the complexity of the strong-coupling method:

a) It is necessary to jointly solve a large number of integrodifferential equations describing both open and closed channels.

b) It is necessary to solve a system of equations with a very small energy step in order to get an accurate picture of the shape of the resonances.

c) An additional numerical fit must be made of the calculated cross section in order to determine the parameters (energies and widths) of the resonances.

### 2.2. Diagonalization method

Far less laborious is the diagonalization method, which was proposed by Balashov *et al.*[25] to describe the resonance ionization of atoms by photons and electrons. This method was subsequently developed to solve problems of the resonance scattering of slow electrons by atoms and ions in Refs. 26–29. In the diagonalization method, the only terms which are retained in expansion (1.7) are those which correspond to open channels $\Gamma'$. Closed channels and the possible capture of the impinging electron by the target are dealt with by adding to the expansion autoionizing-state wave functions which are multiconfiguration functions and which are found from the condition

$$\langle \Phi_\mu \mid H \mid \Phi_\nu \rangle = \varepsilon_\mu \delta_{\mu\nu}. \tag{1.9}$$

In place of (1.7) we then have the expansion

$$\Psi(\Gamma \mathbf{X},\ \mathbf{x}_{N+1}) = (N+1)^{-1/2} \sum_{p=1}^{N+1} (-1)^{N+1-p} \times \sum_{\Gamma'} \Psi(\Gamma' \mathbf{X},\ \hat{r}_p \sigma_p) \frac{F_{\Gamma\Gamma'}(r_p)}{r_p} + \sum_\mu \Lambda_\mu^\Gamma \Phi_\mu(\Gamma \mathbf{x}_1 \ldots \mathbf{x}_{N+1}), \tag{1.10}$$

where the summation over $\Gamma'$ is carried out over open channels exclusively. The functions $F_{\Gamma\Gamma'}$ and the coefficients $\Lambda_\mu^\Gamma$ are the unknown quantities in the problem.

The functions $\Phi_\mu$ are constructed on the basis of the so-called method of superposition of configurations, which is set forth in detail in Refs. 16, 25, and 29, among other places. The functions $\Phi_\mu$ are constructed as a linear combination of single-configuration wave functions of an $(N+1)$-electron system. The configuration mixing coefficients are found from condition (1.9). The basis of configurations from which the functions $\Phi_\mu$ are constructed is chosen in such a way that the functions $\Phi_\mu$ are orthogonal with respect to the open-channel functions which are included in the sum over $\Gamma'$ in (1.10). The functions $\Phi_\mu$ and the energies $\varepsilon_\mu$ thus represent the wave functions and energies of the autoionizing states in the approximation in which the coupling between the open and closed channels is turned off. In the diagonalization method, this coupling is taken into account in first-order perturbation theory; it gives rise to an energy shift of the autoionizing state and to a finite lifetime for these states.

Expansion (1.10) incorporates the closed channels only approximately, since the functions $\Phi_\mu$ decay exponentially with respect to all the variables, while the functions $F_{\Gamma\Gamma'}$ in (1.7) may decay far more slowly, e.g., in a power-law fashion. For this reason, the polarization of the atom by the impinging electron is incorporated in a slightly poorer way by expansion (1.10) than in the strong-coupling method.

On the other hand, the parameters of the autoionizing states may, on occasion, be found even more accurately in the diagonalization method, since it is possible, without any particular difficulty to expand the basis of wave functions from which $\Phi_\mu$ are constructed. We will see an example of this situation in Sec. 8.

Applying the variational principle which we mentioned above to the function (1.10) (both the functions $F_{\Gamma\Gamma'}$ and the coefficients $\Lambda_\mu^\Gamma$ are to be varied), we find the following system of coupled algebraic-integrodifferential equations for determining these quantities (here and below, we replace the channel indices $\Gamma$, $\Gamma'$ by the indices $i, j$, etc.):

$$\sum_{j'} \mathcal{L}_{ij'} F_{j'j} = -\sum_\nu \Lambda_\nu^j U_{i\nu}(r), \tag{1.11}$$

$$(\varepsilon_\mu - E)\,\Lambda_\mu^j + \sum_i \int U_{i\mu}(r)\, F_{ij}(r)\, dr = 0, \tag{1.12}$$

where

$$\mathcal{L}_{ij} = -\frac{1}{2}\left[\frac{d^2}{dr^2} - \frac{l_i(l_i+1)}{r^2} + \frac{2Z}{r} + k_i^2\right]\delta_{ij} + V_{ij} + W_{ij}. \tag{1.13}$$

In (1.13), $V_{ij}$ is the matrix element of the Coulomb interaction between the wave functions of discrete states. Actually, $V_{ij}$ is the potential of the direct interaction of the impinging electron with the target, while $W_{ij}$ is the corresponding potential of the exchange interaction. Explicit expressions for these potentials are given in Ref. 24. The functions $U_{i\mu}(r)$ depend on the particular atom or ion chosen; they are the matrix elements of the Coulomb interaction between the functions $\Phi_\mu$ and the target wave functions.[26,29]

We write the solution of system (1.11) in the form

$$F_{ij}(r) = F^0_{ij}(r) - \sum_\nu \sum_{j'} \int \mathrm{d}r' G_{jj'}(r, r') U_{j'\nu}(r') \Lambda^j_\nu, \quad (1.14)$$

where $F_{ij}$ is a regular solution of system (1.11) without the right side. In (1.14), $G$ is a Green's matrix which satisfies the equation

$$\mathscr{L}_{ij'} G_{j'j}(r, r') = \delta_{ij}\delta(r-r'). \quad (1.15)$$

Substituting (1.14) into (1.12), and assuming that we can ignore the off-diagonal terms

$$\int \mathrm{d}r\, \mathrm{d}r' U_{i\mu}(r) G_{ij}(r, r') U_{i\nu}(r'), \quad \nu \neq \mu, \quad (1.16)$$

in comparison with the diagonal terms, for which we have $\nu = \mu$, we can eliminate $\Lambda^i_\nu$ from (1.11), (1.12). This "diagonalization assumption" [25] is valid in cases in which the resonances are clearly resolvable, i.e., in cases in which the distances between resonances are greater than their widths. This is precisely the situation in the overwhelming majority of cases. It can then be shown[29] that we have

$$T_{ij} = T^0_{ij} + 2i \sum_\mu \alpha_{\mu i}\alpha_{\mu j} \left(E - \varepsilon_\mu - \Delta_\mu + \frac{i}{2}\Gamma_\mu\right)^{-1}; \quad (1.17)$$

here $T^0_{ij}$ are the matrix elements of the nonresonance scattering, and the second term describes the resonance scattering. It is a generalization of the Breit-Wigner formula to the multichannel case. The possibility of explicitly singling out this resonance part is an important advantage of the diagonalization method. The quantities $T^0_{ij}$, like the quantities $\alpha_{\mu i}$, $\Delta_\mu$ and $\Gamma_\mu$ are expressed in terms of the solutions $(F^0_{ij})$ of system (1.11) without its right side, i.e., the solutions of the system of equations of the strong-coupling method in which closed channels are not considered. The quantities $\Delta_\mu$ represent the shifts of the resonant energies $\varepsilon_\mu$ due to the interaction of the discrete states $\Phi_\mu$ with the adjacent continuum. The total widths of the resonances are

$$\Gamma_\mu = \sum_i \Gamma_{\mu i}, \quad \Gamma_{\mu i} = |\alpha_{\mu i}|^2, \quad (1.18)$$

where $\Gamma_{\mu i}$ is the partial width of resonance $\mu$ which stems from its decay into channel $i$.

We thus see that in the diagonalization method, as in the strong-coupling method, there is an approximate dynamic description of the resonance scattering. In other words, the parameters of the resonances are described in terms of an initial Hamiltonian, without the introduction of any arbitrary adjustable parameters.

### 2.3. *R*-matrix method

In the diagonalization method described above, the Hamiltonian is diagonalized in the subspace of closed channels through solution of a system of algebraic equations, while its diagonalization in the subspace of open channels requires solving a system of integrodifferential equations. Also widely used in the theory of electron-atom collisions is a method for solving the system of strong-coupling equations in which the problem of diagonalizing the Hamiltonian in the space of both closed and open channels essentially reduces to a system of algebraic equations. This is the "*R*-matrix method."

The basic idea of this method is to partition the configuration space of the $(N+1)$-electron system consisting of the atom plus the electron into two parts: an inner part $r < a$ and an outer part $r > a$, where $a$ is the distance from the center of the atom to the electron. The radius of the inner part, $a$, is chosen as small as possible under the restriction that all the radial wave functions $P_{nl}(r)$ of the atomic electrons must vanish with the required accuracy at $r > a$. Let us examine the solution $(U_i)$ of the system of equations of the strong-coupling method in the region $r < a$ under the boundary conditions

$$U_i(0) = 0, \quad a\frac{\mathrm{d}U_i(r)}{\mathrm{d}r}\Big|_{r=a} = BU_i(a), \quad (1.19)$$

where $B$ is some arbitrary fixed real number (e.g., zero). It turns out that solutions of this sort exist only for certain discrete values $E_\lambda$ of the energy of the system. We denote these solutions by $U_{i\lambda}$. A method for finding $U_{i\lambda}$ is described in Ref. 30, among other places. The idea of this method is to write the functions $U_{i\lambda}$ as linear combinations of known functions $U^0_\nu$ which satisfy the same boundary conditions as the function $U_{i\lambda}$. The functions $U^0_\nu(r)$ describe the radial motion of an electron in a potential field $V(r)$ which serves as a model of the target field. The problem of finding $U_{i\lambda}$ then reduces to one of solving a system of algebraic equations for the expansion coefficients. It can then be shown[30] that the values of the functions $F_{ij}$ and their derivatives at the boundary $r = a$ are related by

$$F_{ij}(a) = \sum_{i'} R_{ii'}(B, E)\left(a\frac{\mathrm{d}F_{i'j}}{\mathrm{d}r} - bF_{ij}\right)_{r=a}, \quad (1.20)$$

where the $R$-matrix is

$$R_{ij}(B, E) = \frac{1}{2a}\sum_\lambda \frac{U_{i\lambda}(a)U_{j\lambda}(a)}{E_\lambda - E}. \quad (1.21)$$

Once the $R$-matrix has been found, it is a simple matter to find the solution $(F_{ij})$ of the system of integrodifferential equations in the outer region which satisfies the given asymptotic condition. In the outer region, all the short-range and exchange potentials are zero, so that it is a simple matter to find a complete set of linearly independent particular solutions in this region. The solution being sought, $F_{ij}$, can then be written as a linear combination of these particular solutions, and the coefficients of the linear combination can be found from condition (1.20) and the asymptotic condition in the limit $r \to \infty$.

We have two comments here. First, although the $R$-matrix does depend on the particular choice of the constants $a$ and $b$, observable quantities do not depend on them. Second, the $R$-matrix method has the important advantage that the $E$ dependence of the $R$-matrix is present only in the denominator, as can be seen from (1.21), so that it is a trivial matter to find it for various values of $E$ once the values of $U_{i\lambda}(a)$ are known.

We might also mention some other theoretical methods, which have been used comparatively infrequently to study resonance phenomena in electron collisions. Examples are the quantum-defect theory, the random phase approximation with exchange and an algebraic variational method.[34] We will not discuss these methods in any detail here; we refer the interested reader to Refs. 31–34.

The quantum-defect theory has been used to study series of resonances in electron-ion collisions which converge on various excited states of the cerium ion. In that method, as in the $R$-matrix method, configuration space is partitioned into two regions. In the outer region, the wave function of the scattered electron is taken to be a purely Coulomb wave function, while in the inner region it is constructed with the help of a quantum defect.[31] Despite the simplicity of this method, it leads to some fairly accurate results in cases in which the resonances lie near the threshold.

The random phase approximation with exchange is a version of the perturbation method in many-body theory. It uses a summation of certain sequences of diagrams to calculate the amplitudes of various processes in electron-atom collisions. The intermediate states in the random phase approximation with exchange, however, are taken to be particle-hole states, so that this method can describe only shape resonances and resonances in processes in which atoms are ionized by electrons which are caused by autoionizing states. These autoionizing states form in a one-electron excitation of inner shells of the atom. In order to describe the Feshbach resonances which result from two-electron excitations, it is necessary to generalize the random phase approximation with exchange to incorporate (two-particle)-(two-hole) states among the intermediate states. This generalization was recently carried out and applied to the ionization of atoms in Refs. 33 and 35.

In summary, several theoretical methods are available which, as we will see below, give a good quantitative description of the scattering of electrons by atoms and ions at low energies and can furnish accurate values of the parameters of low-lying resonances. The high-lying resonances, at energies at which there are many open channels, at present lie beyond the capabilities of existing theoretical methods.

## 3. EXPERIMENTAL METHODS

Let us briefly examine the most common methods for experiments on resonances in the scattering of electrons by atoms and ions.

In experiments on resonances in electron-atom collisions, a monoenergetic electron beam is scattered either as it passes through a gas in a collision chamber or as it intersects an atomic beam. Information on the resonances in electron-ion collisions is obtained from experiments with intersecting beams of electrons and ions. There are four basic types of experiments, depending on what is detected after the scattering. In experiments of the first type ("electric" experiments), the electrons are detected. In experiments of the second ("optical") type, the radiation from the atom or ion excited as a result of the collision is detected. If the lifetime of the excited atom or ion is longer than the time required for the atom or ion to travel to the detector, one can resort to experiments of a third type: detecting the atoms or ions in a metastable excited state ("the metastable-spectroscopy method"). The experiments of the fourth type make use of a

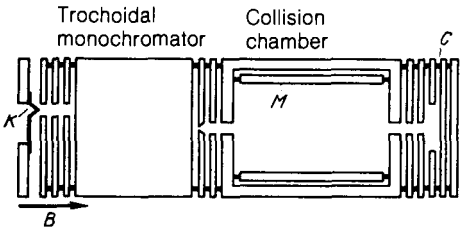


FIG. 1. Layout of a transmission experiment.[38]

coincidence technique. In these experiments, various pairs of particles which are products of the collision may be selected as the particles to be detected.

In most cases, the resonances have a width of $10^{-1}$–$10^{-3}$ eV or less. In order to detect a resonance, it is thus necessary to produce an electron beam in which the energy spread of the electrons is of the same order of magnitude. The quantity usually adopted as a measure of the energy spread of the beam is $\Delta E$, the width of the electron energy distribution at half-maximum. We will refer to $\Delta E$ as simply the "energy spread" of the beam.

The Pierce electron guns which are ordinarily used provide an energy spread $\sim 0.3$ eV at best. In order to achieve a narrow energy distribution, one should therefore use electron velocity selection. Monochromators with various electric and magnetic field configurations are used for this purpose. The monochromators which are presently used most extensively are the trochoidal electron monochromator (Fig. 1), which operates in a longitudinal magnetic field of 100–200 Oe, and electrostatic monochromators, a 127° cylindrical monochromator (Fig. 2) and a 180° hemispherical monochromator. In the latter two monochromators the electric field is produced between cylindrical or spherical surfaces of certain radii. These monochromators have furnished beams with an energy spread $\sim 20 - 40$ meV.

Monoenergetic electrons can also be produced through the photoionization of atoms by monochromatic light. Stumpt and Gallagher[36] used this approach to produce an electron beam with $\Delta E = 7$ meV, which they used to study resonances in electron scattering by inert gas atoms. There is reason to believe that this method could be pursued to achieve an energy spread[37] $\Delta E \sim 1$ meV.

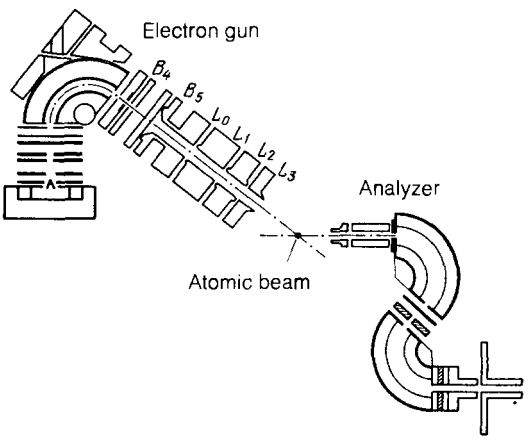


FIG. 2. Layout of Eyb and Hofmann's spectrometer.[39]

Another important characteristic of an electron beam is its current $I_0$. As this current is raised (at a given electron energy), the number of electron-atom collisions per unit time increases, as does the ratio of the useful signal to the background. On the other hand, an increase in the current increases the space charge density in the beam, which in turn degrades the energy spread $\Delta E$ along the path over which the beam is transported to the collision chamber. A cylindrical monochromator has furnished a beam with $\Delta E \sim 20$ meV at a current $I_0 \sim 10^{-8}$ A.

Experiments of the "electric" type have been carried out in various ways, depending on which cross section is to be measured. We will briefly describe some versions of this method.

The total cross section for the interaction of electrons with atoms is measured in a "transmission" experiment: an experiment on the passage of an electron beam through a gas. Figure 1 shows the arrangement for an experiment of this type, which was refined by Sanche and Schulz.[38] A beam of electrons emitted by cathode $K$ goes to the input of the trochoidal monochromator, within which the longitudinal magnetic field **B** performs a velocity selection on the electrons. At a current of $5 \cdot 10^{-9}$ A the energy spread is 30 meV. After the electrons have been accelerated to the desired energy, they are sent into a collision chamber which is filled with a gas to a pressure of $10^{-2}$ Torr. Those electrons which pass through the gas and are not scattered strike collector $C$. Those electrons which are lost as a result of collisions are retarded by the potential of an electrode in front of the collector. Also incident on the collector, of course, are electrons which have undergone a forward elastic scattering, but they can be ignored if the geometry is chosen appropriately. The current $I$ drawn by the collector is then related to the current at the entrance to the collision chamber, $I_0$, by

$$I = I_0 e^{-Nl\sigma}, \tag{2.1}$$

where $\sigma$ is the total interaction cross section which is being sought, $l$ is the distance traversed by the electron in the collision chamber, and $N$ is the number of atoms per unit volume. Relation (2.1) can thus be used to find $\sigma$ from the measured current $I$ and the known values of $I_0$, $N$, and $l$.

The sensitivity of the experiment is improved by modulating the energy of the electron beam by a small alternating voltage of 0.005–0.06 V, which is applied to cylinder $M$ inside the collision chamber. The scattering signal, which is proportional to the derivative of the cross section with respect to the energy is distinguished at the modulation frequency by a lock-in detector. Since we have $\Delta I / I = Nl\Delta\sigma$, and since the relative change $\Delta I / I$ upon a change in the energy of the electron beam is larger than the relative change in the cross section, $\Delta\sigma/\sigma$, by a factor of $\sigma Nl$, this method can effectively distinguish the changes caused in the cross section by the resonances from the slowly varying background under the condition $\sigma Nl > 1$.

Experiments carried out to measure the total cross section do not provide information which would be of assistance in classifying the resonances, i.e., in determining the configuration, the total angular momentum $L$, and the total spin $S$ of the autoionizing states. Information of this sort is provided by experiments in which the differential cross section is measured for some type of elastic or inelastic scattering of an electron. For example, if the atom has a zero orbital angular momentum in its initial and final states, the total angular momentum $L$ is equal to the angular momentum of the scattered electron, $l$, and the angular dependence of the differential cross section at the resonance energy is determined primarily by the angular dependence of Legendre polynomial $P_l$. The $P$-resonance, for example, is seen most clearly at the scattering angles $\theta = 0°$ and 180° and is not observed at all at $\theta = 90°$, since $P_1(\cos\theta) = \cos\theta$.

Electron spectrometers are used to measure the differential cross section for electron scattering by atoms. An electron spectrometer is a combination of an electron monochromator and analyzer. The monochromator produces a monoenergetic electron beam. The electrons which are scattered through a certain angle in the collision chamber, and which have the energy to which the analyzer is tuned, pass through the analyzer and are detected. The electron analyzer operates on the same principle as the monochromator; i.e., an electric or magnetic field performs an energy selection on the scattered electrons.

Figure 2 shows the typical spectrometer layout which Eyb and Hofmann[39] used to study the scattering of electrons by atoms of alkali elements.

The electrons from the electron gun are focused by a system of lenses onto the entrance to a 127° cylindrical monochromator. After the energy selection, the electrons are focused onto an atomic beam by the lens system $B_4$–$L_3$. The double 127° cylindrical analyzer can be rotated around the atomic beam between $-100°$ and $+150°$. The analyzer should pass those electrons which are scattered through a certain angle and which have a certain energy. The analyzer is accordingly put in the appropriate position, and the scattered electrons are accelerated to the energy which will be passed by the analyzer and focused by a system of lenses onto the entrance to the analyzer. Those electrons which have passed through the analyzer are accelerated and focused onto an electron multiplier by a lens (at the bottom right in Fig. 2). The angular resolution of the spectrometer is $\pm 1.5°$, while the energy resolution is about 70 meV.

At a fixed energy of the incident electrons and at a fixed scattering angle, it is also possible to measure the dependence of the number of scattered electrons on the energy which they lost in collisions; i.e., it is possible to measure a loss spectrum.

The electric methods in which the changes which occur in the electrons impinging on the target can be used to study only low-lying resonances, since the resolution of the best electron spectrometers is $\approx 20$ meV, and the resonances become progressively more closely spaced as the energy increases. An optical method is free of this shortcoming.

An optical method involves studying the optical excitation functions of the spectral lines of the radiation from an atom. These functions are measured with a high resolution in terms of the energy of the impinging electrons, achieved through the use of the same monochromators for the impinging electrons as in the electrical methods. As a rule, the radiation from the collision chamber is brought out at right angles with respect to the electron beam. A system of lenses then directs the radiation to a spectral instrument which selects the radiation at the wavelength of interest.

We turn now to electron-ion scattering. The most reliable experimental data on the scattering of electrons by ions are obtained in experiments of an optical type involving in-

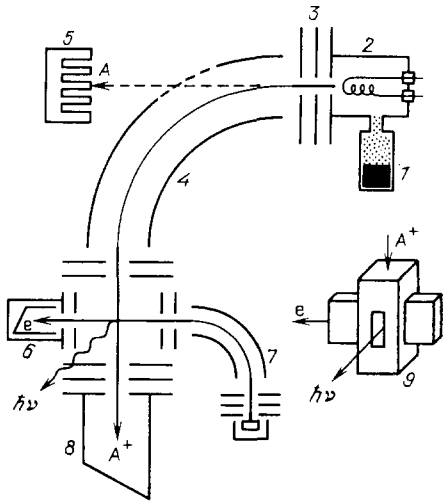


FIG. 3. Layout of an experiment with intersecting beams of ions and electrons.[40]

tersecting electron and ion beams. However, several difficulties confront efforts to determine experimentally the excitation cross sections in beam experiments. The greatest difficulty is the mutual effect of the space charge of the beams. Furthermore, since the ion density in the beam is usually $\sim 10^6$–$10^7$ cm$^{-3}$, which is well below the residual gas density in the collision chamber, the yield of reaction products (usually, photons) must be detected in the face of a significant background signal, whose level is sometimes two orders of magnitude greater than the useful signal. It thus becomes necessary to arrange an ultrahigh vacuum in the collision chamber in the face of a continuous influx of working medium into this chamber ($\sim 10^{-8}$ Torr).

Figure 3 shows the layout of an experiment[40] carried out to study the cross sections for the excitation by electrons of ions of alkaline earth elements.

Beams of positive ions are produced by a source in which atoms can be ionized in two ways. The first method is a surface method, in which atoms from heated reservoir 1 diffuse into chamber 2 and are ionized on the surface of a hot cathode. In the second method, the ions are formed in the arc of a low-voltage discharge between the cathode and the front wall of the ionization chamber. The density of the ion beam can be adjusted up to $6\cdot 10^{-5}$ A/cm$^2$.

The ions which are produced are extracted from the ionization chamber, accelerated, and formed into a beam by ion-optics system 3, which consists of three lenses. The ions then undergo an energy selection and are separated from the atoms in 90° electrostatic capacitor 4. Part of the outer plate of the capacitor is made of a tungsten grid, which is transparent to the atoms, which diffuse out of the source and are captured by trap 5. In the collision chamber, the ion beam intersects the electron beam and then goes to Faraday cup 8.

A beam of monoenergetic electrons is produced by a 90° cylindrical electrostatic monochromator 7 and then strikes collector 6. The current density of electrons with energies in the interval 2–20 eV ranges from $2.5\cdot 10^{-5}$ A/cm$^2$ to $6.0\cdot 10^{-4}$ A/cm$^2$. The energy spread of the beam is varied over the interval 100–300 meV. The cross sections of the ion and electron beams are 6.25 and 0.3 mm$^2$, respectively.

The radiation from the collision region is incident on a monochromator with a diffraction grading at an angle of 90° from the collision plane. This radiation is detected by a photomultiplier operated in the photon-counting mode. The useful signal is discriminated from the background due to the excitation of ion states in collisions of ions with neutral atoms of the residual gas and of the working medium by a method involving a modulation of both beams with square pulses, which are out of phase by 1/4 of a period. The pulsed signal is detected in two counting channels, which are switched in synchronism with the modulation pulses.

The energy spread which has been achieved to date for the ion and electron beams is not sufficient for detecting individual resonances in electron-ion collisions. The structural features which are seen in the cross sections are actually consequences of an average resultant contribution of series of resonances.

The method of metastable spectroscopy can be used to measure either the total or differential cross sections for the excitation of metastable states. A description of this method is given in Ref. 41, where the differential cross sections for the excitation of metastable states of inert gas atoms were measured. In those experiments, an intense atomic beam [$\sim 10^{15}$ atoms/cm$^2\cdot$s] $\sim 2$ mm in diameter was produced by a gas dynamic source with the help of a supersonic nozzle. The angular divergence of the beam was $< 1°$, and the energy spread was $\sim 60$ meV for He or $\sim 50$–$80$ meV for Ne, Ar, Kr, and Xe. The atomic beam intersected the electron beam ($\Delta E < 80$ meV) at right angles; the electron beam was formed by an electrostatic 127° monochromator. The atoms in a metastable state which were formed as a result of collisions with electrons recoiled, deviated from their original direction of motion, and formed a broad angular distribution. This angular distribution was measured with a channel electron multiplier, which was placed at various observation angles. At each fixed value of the electron energy, the angular dependence of the intensity of the beam of metastable atoms was measured. Important data were obtained on structural features, including resonances, in the cross sections.

The coincidence technique has been used most extensively in so-called (e,2e) experiments on the electron-impact ionization of atoms. In these experiments, the scattered and emitted electrons are detected in coincidence. Since the energies and directions of motion of the scattered and emitted electrons are measured in these experiments, they completely determine the kinematics of the process. As Balashov *et al.* have shown,[42] measurements of this type can be used to obtain information on ionization through the excitation of autoionizing states of an atom and on the symmetry of the autoionizing states themselves.

Coincidence experiments have recently been extended to the study of the excitation of atoms by electrons.[43] In these so-called (e,e'$\gamma$) experiments both the electron which excites the atom and which is scattered through a certain angle and the photon emitted in a certain direction by the excited atom are detected. Experiments of this sort require an apparatus with a high time resolution (of the order of 1 ns). The requirements of a small energy spread of the electron beam naturally remain in force in a study of resonances. Photon-electron coincidence experiments make it possible to study the amplitudes for the excitation of sublevels of a given level

which are degenerate in the magnetic quantum number (so-called coherent excitation).[44]

Another rapidly developing approach in experiments on electron-ion collisions is that of experiments with polarized beams of atoms and electrons. The information obtained from such experiments turns out to be very useful for classifying resonances. We will discuss polarization experiments in more detail in Sec. 10.

In concluding this section of the paper we note that most of the experimental effort has been aimed at determining total cross sections. So far, very little work has been carried out to determine differential cross sections or using polarized beams.

## 4. HYDROGEN ATOM

The hydrogen atom is the darling of the theoreticians. Unfortunately, the scattering of electrons by hydrogen atoms is difficult to study experimentally because of the complexity of producing atomic hydrogen. It is thus not surprising that the scattering of electrons by the hydrogen atom was studied in great detail theoretically before corresponding experiments were carried out. However, it was only in 1962, in calculations carried out by the method of strong channel coupling by Smith *et al.*,[45] that it was found that the total elastic cross section increases very sharply below the excitation threshold for the $n = 2$ level of the H atom, because of a rapid increase in the $^1S$ and $^3P$ scattering phase shifts. Similar results were obtained nearly simultaneously by Burke and Shey,[2] who worked from a detailed study of the behavior of the scattering phase shifts near the threshold to predict the existence of a $^1S$ resonance at an energy $E = 9.61$ eV with a width $\Gamma = 0.109$ eV. Burke *et al.* subsequently refined the values of the parameters of this resonance; in Ref. 46 they found $E = 9.56$ eV and $\Gamma = 0.0474$ eV, which are the values generally accepted today.

Gaĭlitis and Damburg[3] proposed an explanation for the mechanism for the formation of resonances in cross sections for the scattering of electrons by hydrogen atoms. They started from the position that although an atom in a state with a definite parity does not have a dipole moment there can be states with a definite energy and an indefinite parity, with a nonzero dipole moment, in a case in which degenerate levels exist. An example of such a state might be the $(2s + 2p)/\sqrt{2}$ state of the H atom. The attractive potential of the atom in this state has an $\alpha/r^2$ asymptotic behavior. Gaĭlitis and Damburg showed that in the case of hydrogen the value of $\alpha$ would be such that in the field $\alpha/r^2$ there could be a set of bound states, which convert into autoionizing states when the coupling with an open channel is taken into account. In this case the system of levels of the $H^-$ ions would consist of infinite series of doubly excited states. Each such series would be characterized by a certain value of the principal quantum number $n$ of that level of the H atom to which the given series converged and by the several possible values of the total orbital angular momentum at the given value of $n$. Each level of the series is therefore characterized by the quantum numbers $n = 2$, $L = 0$–$2$; $n = 3$, $L = 0$–$4$; $n = 4$, $L = 0$–$6$; etc. The energies of the levels converging on the ionization level form a geometric progression.

The first experimental confirmation of the existence of a resonance near 9.6 eV was found by Schulz[47] in a 1964 transmission experiment in which an electron beam with an energy below 10.2 eV passed through partially dissociated hydrogen. Schulz found a resonance energy $E = 9.77 \pm 0.15$ eV, but the poor energy spread of the electron beam (0.3 eV) prevented a determination of the width of the resonance. In subsequent experiments carried out by Kleinpoppen and Railbe[48] and also by McGowan *et al.*,[49] with electron beams with a better energy spread ($\sim 0.08$ eV)—achieved through the use of a 127° electrostatic selector—structure in the cross section was also observed near 9.6 eV.

Furthermore, some additional structure was observed in the elastic cross section below the $n = 2$ threshold of the H atom in Ref. 49. The results found in Ref. 49 were analyzed in Ref. 50 by the method of strong channel coupling. The differential cross section for elastic scattering through an angle of 90° was calculated; the low-lying $^1S$ and $^1D$ resonances were taken into account. The results of these calculations showed that the $^1D$ resonance ($E = 10.126$ eV, $\Gamma = 0.0088$ eV) was responsible for the peak in the cross section below the $n = 2$ threshold. Recent measurements of the differential elastic cross section with an electron beam with a very small energy spread ($\sim 25$ meV) at energies $< 10.2$ eV confirmed the presence of a complicated resonance structure due to $^1S$, $^1D$, and $^3P$ resonances[51] (Fig. 4).

Resonances in the excitation cross sections of the hydrogen 2s and 2p levels have been the subject of several experimental (e.g., Ref. 52) and theoretical[53] studies. The cross sections $\sigma_{1s\text{-}2s}$ and $\sigma_{1s\text{-}2p}$ are characteristically finite at the threshold and have a shape resonance at $E = 10.2207$ eV with a width $\Gamma = 0.02$ eV (Ref. 53). However, it was only in the mid-1970s that it became possible to compare the theoretical and experimental results, when an energy spread $\Delta E = 16$ meV was achieved for electron beams. Figure 5 shows theoretical and experimental excitation cross sections of the 2s level of the hydrogen atom. The vertical lines mark

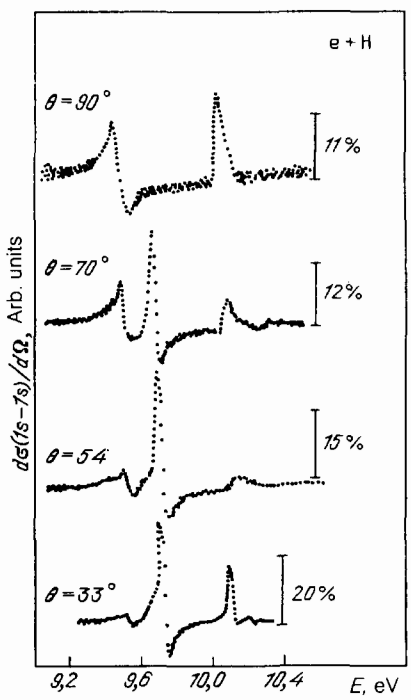


FIG. 4. Differential cross section for elastic e + H scattering.[51] The vertical bars show the height of the resonance features with respect to the direct scattering process.

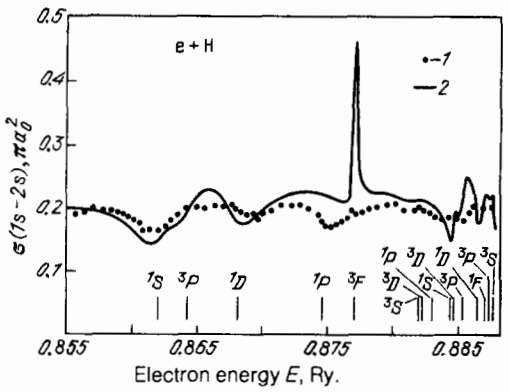


FIG. 5. Total cross section for electron-impact excitation of the 2S level of H. 1—Experiment of Ref. 52; 2—calculation of Ref. 53.

the calculated positions of the resonances. The absolute values of the experimental cross sections were measured within an error of 15–17%. Although the theoretical cross section shown in Fig. 5 has not been averaged over the energies of the beam electrons, we see that there is qualitative agreement between the theoretical and measured cross sections.

On the whole, hydrogen is a subject which defies the experimentalists. The experimental difficulties in working with atomic hydrogen have yet to be completely overcome. So far, the extensive theoretical calculations of resonances have not received a detailed quantitative experimental confirmation because of the large energy spread of the electron beams. A beam energy spread $\Delta E \sim 1$ meV would be desirable here.

## 5. HELIUM ATOM

Around 1962, Schulz took up the study of the elastic scattering of electrons by helium atoms. His goal was to study the so-called Wigner cusps, i.e., the slope changes in the elastic cross section at energies corresponding to the thresholds for inelastic processes. Since the first inelastic-scattering channel opens up at an energy of 19.8 eV, Schulz focused on specifically this energy region. He in fact observed a broad dip in the differential cross section for elastic scattering through an angle of 72° at this energy. However, after he carefully calibrated his energy scale, it turned out that the structural feature which was observed occurred at an energy of 19.3 eV, i.e., 0.5 eV below the $2^3S$ threshold, so that it could not be a Wigner cusp.[4] A subsequent analysis based on theoretical calculations showed that this structural feature was a resonance due to the existence of a quasibound state of the negative $He^-$ ion with the $1s2s^2\ ^2S$ configuration. Since then, several teams have carried out precise measurements to determine the $1s2s^2\ ^2S$ resonance. The results of these experiments are listed in Table I.

The most accurate theoretical calculations on the elastic scattering e + He were carried out by the $R$-matrix method by Burke *et al.*,[54] who took into account eleven states of He ($1^1S$, $2^{1,3}S$, $2^{1,3}P^0$, $3^{1,3}S$, $3^{1,3}P^0$, and $3^{1,3}D$). As can be seen from Table I, the theoretical results are in excellent agreement with the theoretical parameter values of the resonance. Subsequent experiments were carried out to detect other resonances caused in elastic e + He scattering by high-lying autoionizing states which converge on the $n = 2$ thresholds of He. The most abundant data were obtained by Golden,[55] who observed thirteen resonance features in the energy interval 19.3–21.3 eV (Fig. 6), five of which lay below the $2\ ^3S$ threshold. In these experiments, the derivative of the current with respect to the electron energy was measured. It was this circumstance—as was mentioned in Sec. 2—which made it possible to reveal clearly the resonance features in the cross section. So far, there are no theoretical data which confirm this resonance structure; furthermore, some more recent experiments[56] have failed to confirm the resonance structure observed in the cross section by Golden.

The inelastic scattering of electrons by helium atoms, in particular, the excitation of the $2^{1,3}S$ and $2^{1,3}P^0$ levels of He, is of much theoretical and experimental interest. Several studies have been carried out on resonances in the excitation cross sections.[57,58] These studies have revealed structure in the cross sections which stems from both closed-channel resonances and shape resonances.

The excitation functions of the 3, 4, $5\ ^{1,3}S$, and $6\ ^1S$ levels of He were measured in Ref. 57 at energies from 22.5 eV up to the ionization threshold ($E = 24.54$ eV). These measurements revealed $1sns^2\ ^2S$, $nsnp^2\ ^2P$, and $1snp^2\ ^2D$ and $^2S$ resonances. Some high-resolution experiments were recently carried out on the excitation of the $2\ ^3S$ and $2\ ^1S$ levels at energies from 19.8 eV to 22.7 eV (Ref. 59). The results of those experiments are shown in Fig. 7, where they are compared with the most accurate theoretical calculations.[54]

Experimentalists have recently been showing progressively more interest in determining the excitation functions of atoms for excitation from excited states, in particular, metastable states. Optical excitation functions of this sort for He were recently studied by Heddle, Keesing, and Kurepa.[60] They determined the functions of the $4^3S$–$2^3P$, $4^1S$–$2^1P$, etc., transitions. A resonance structure was also seen on many of these functions.

Table II shows the results of measurements of the energies of resonances by various methods. It can be seen from Table II that at present there are some significant experimental discrepancies regarding the existence of many resonances and also their energy positions. Since we lack accurate experimental data, the existence of many of these resonances should be regarded as an open question at this point. For example, Massey[61] believes that only eight states of $He^-$ can

TABLE I. Parameters of the $1s2s^2\ ^2S$ self-detaching state of $He^-$

| | Theory | | | Experiment | | |
|---|---|---|---|---|---|---|
| | Ref. 166 | Ref. 175 | Ref. 167 | Ref. 55 | Ref. 174 | Ref. 168 |
| $E$, eV | 19.38 | 19.37 | 19.376 | 19.35±0,02 | 19.367±0.009 | 19,37 |
| $\Gamma$, meV | 15.1 | 11.72 | 11.56 | 13.0 | 9.0±1 | 9.0 |

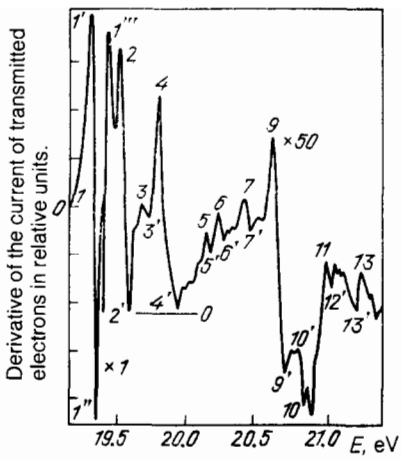


FIG. 6. Derivative with respect to the energy of the current of electrons passed through helium as a function of the electron energy according to the experiment of Ref. 55.

be regarded as reliably identified states of the negative $He^-$ ion which lie below the ionization threshold.

Resonances in the scattering of electrons by atoms of other inert gases are the subject of a huge literature. However, most of this work concerns resonances which arise upon the excitation of an electron from inner shells or upon the excitation of two electrons from an outer shell. In Ref. 62, for example, a study was made of resonances which stem from autoionizing states with the configurations $[nsn1p^6]mlm'l'$ and $[ns^2np^4]mlm'l'm''l''$. Since resonances of this type go beyond the scope of this review, we refer the reader to the original paper[62] (see also Refs. 63 and 64 and the references there). The method of metastable spectroscopy (Sec. 3) was used in Ref. 41 to measure the total and differential excitation cross sections of metastable states of Ne, Ar, and Kr atoms. Resonances were detected. In the scattering of electrons by the Ne atom, for example, a resonance $2p^5(^2P_{3/2,1/2})3s3p\ ^3P$ was observed at an electron energy of 16.91 eV and a resonance $2p^5(^2P_{3/2,1/2})3p^2\ ^1S, ^1D$ was observed at 18.67 eV. Read[65] has recently published a detailed review of experiments carried out to detect resonances in the low-energy scattering of electrons by inert gas atoms. On the theoretical side, calculations were carried out in Ref. 66 on the resonance scattering of electrons by inert

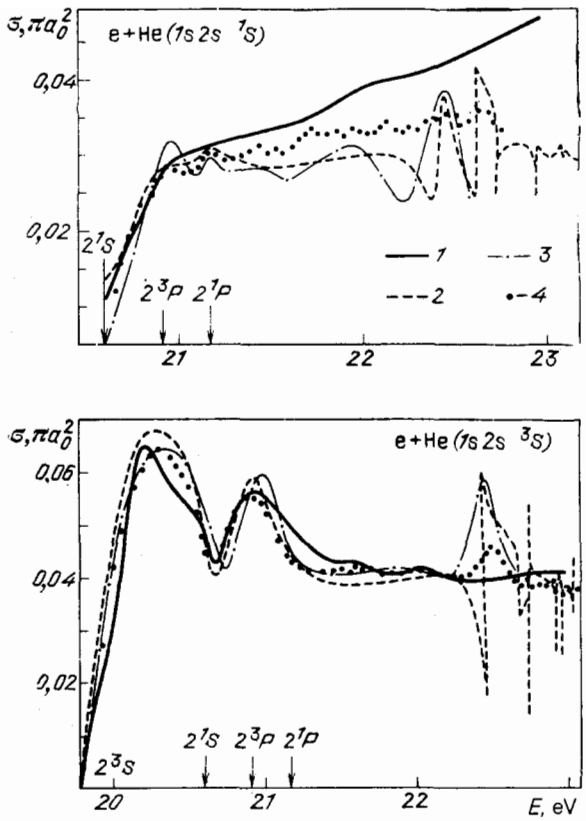


FIG. 7. Comparison of theoretical and experimental excitation cross sections for electron-impact excitation of the 1s2s $^{1,3}S$ levels of He. 1—Calculations of Ref. 166; 2—calculations of Ref. 54; 3—calculations of Ref. 173; 4—experiment of Ref. 59.

gas atoms. The results of the calculations agree well with the experimental data.

## 6. HELIUM ION

The resonance structure in the electron scattering cross sections of the helium ion, which is isoelectronic with the hydrogen atom, is significantly richer than that for the hydrogen atom, because of the presence of a long-range attractive Coulomb potential.

The first experimental study of the excitation cross section of a level of $He^+$ in excitation by electrons was carried

TABLE II. Energies of the resonances in e + He scattering found in various experiments.[19]

| Notation in Fig. 6 | Ref. 55 | | | Ref. 38 | | Ref. 169 | | Ref. 5 | | Ref. 170 | Ref. 171 | Classification[55] | Energy of state[55] |
|---|---|---|---|---|---|---|---|---|---|---|---|---|---|
| | Max. | Zero | Min. | Max. | Min. | Max. | Min. | Max. | Min. | | | | |
| 1–1′–1″–1‴ | 19,32<br>19,43 | 19,34 | 19,36 | 19,37 | 19,30 | 19,30 | 19,40 | 19,31 | 19,37 | | 19,30 | $2\ ^2S$ $He^-$ | |
| 2–2′ | 19,51 | | 19,55 | | | 19,43 | 19,47 | 19,43 | 19,47 | | | $2\ ^2P$ $He^-$ | |
| 3–3′ | 19,69 | | 19,73 | | | 19,58 | 19,62 | | | | | | |
| 4–4′ | 19,825 | | 19,93 | 19,80 | 19,80 | 19,818 | | 19,818 | | | | $2\ ^3S$ He | 19,818 |
| 5–5′ | 20,10 | | 20,14 | | | 20,04 | 20,10 | | | | | | |
| 6–6′ | 20,23 | | 20,27 | | | 20,17 | 20,21 | | | | | | |
| 7–7′ | 20,40 | | 20,44 | | | 20,30 | 20,35 | | | | | | |
| 8–8′ | 20,45 | | | | | | | | | 20,34 | 20,45 | $2\ ^2P$ $He^-$ | |
| 9–9′ | 20,61 | | 20,69 | 20,58 | 20,62 | 20,59 | | 20,59 | | | | $2\ ^1S$ He | 20,614 |
| 10–10′ | 20,86 | | 20,82 | | | | | | | | | | |
| 11–11′ | 20,98 | | | | | 20,93 | 21,22 | | | | | $2\ ^3P$ He | 20,962 |
| 12–12′ | | | 21,02 | | | | | | | 20,99 | 21,00 | $2\ ^2D$ $He^-$ | |
| 13–13′ | 21,24 | | 21,19 | | 21,19 | | | | | | | $2\ ^1P$ He | 21,216 |

out in 1966 by Harrison *et al.*[67] by the method of intersecting beams. Although the energy spread of the electron beam was $\sim 1.5$ eV a broad maximum was detected in the cross section at an energy of 48 eV even in this first experiment.

The most careful experiment on the excitation of the 2s level of $He^+$ was carried out by Peart and Dolder,[68] who used a method analogous to that of Ref. 67. The resonance structure found in the cross section of their experiment agrees well in terms of shape with both the experimental data of Ref. 67 and the calculated data of Ref. 69.

An experimental study of the excitation of the 2p level of $He^+$ was undertaken in 1974 at Uzhgorod University by a team lead by Zapesochnyĭ.[70,71] They used an apparatus with modulated intersecting electron and ion beams. The efficiency of the level excitation was found by measuring the radiation at the wavelength $\lambda = 304$ Å which appeared in the transition $1s\ ^2S_{1/2} - 2p\ ^2P^0_{1/2,3/2}$. These first experiments did not reveal structure in the excitation function. The first experimental indication of the existence of resonances in the excitation cross section of the 2p level of $He^+$ in the region 45–55 eV appeared in Ref. 6. In the very recent experiment of Ref. 72 a clearly defined resonance structure was found in the cross section. This structure consisted of broad maxima, two of which lay below the $n = 3$ threshold of $He^+$.

On the theoretical side, the calculations on resonances in the e-$He^+$ scattering cross sections have been carried out by the method of strong channel coupling (see, e.g., Ref. 69 and the references there), by the method of strong channel coupling with correlation functions,[46,73] by the algebraic variational method,[74] and by the diagonalization method.[26,29]

Figure 8 shows theoretical and experimental total cross sections for the excitation of the 2s level of $He^+$. We see that the results calculated by the method of strong channel coupling with correlation functions and by the diagonalization method agree well. A particularly good agreement was achieved for the position and shape of the first deep minimum in the cross section, at an energy of 44.8 eV; this minimum stems from low-lying $^1S$ and $^3P^0$ autoionizing states of He. In the nonresonance region, in contrast, the cross section found by the diagonalization method is 25% larger than that calculated by the method of strong channel coupling with correlation functions. The reason is that the polarization of the target caused by the higher-lying states is not taken into account as thoroughly in the diagonalization method as it is in the method of strong channel coupling with correlation functions. A comparison of the theoretical and experimental cross sections shows that the theoretical cross sections are significantly larger (by a factor $\sim 1.5$–2). Henry's recent analysis[76] of the reasons for such a large discrepancy shows that the experimental cross section reported in Ref. 75 is apparently substantially too low, because of difficulties in the normalization of the experimental curve. At the same time, the cross section found by the diagonalization method and averaged over the distribution of the electrons in the beam, 1.5 eV wide (chosen in accordance with the conditions in the experiment of Ref. 68), agrees well with the experimental cross sections in terms of shape. This result shows that the electron-electron correlation interaction which is responsible for the resonance effect is taken into account quite accurately in the calculations by the diagonalization method.

Figure 9 shows theoretical and experimental excitation cross sections for the resonance 2p level of $He^+$. Comparison of the cross section calculated by the diagonalization method and integrated with a Gaussian distribution function 1.5 eV wide, on the one hand, with the experimental cross section[72] (Fig. 9) on the other, shows that the calculated cross section agrees well with the experimental cross section in terms of shape (in the energy interval between the $n = 2$ and $n = 3$ thresholds of $He^+$), although the calculated cross section is slightly larger. Consequently, the resonance structure observed in the cross section in Ref. 72 can be explained entirely in terms of an Auger decay of an autoionizing state of He, which converges on the $n = 3$ and $n = 4$ thresholds of $He^+$.

In a recent study,[156] the method of strong channel cou-

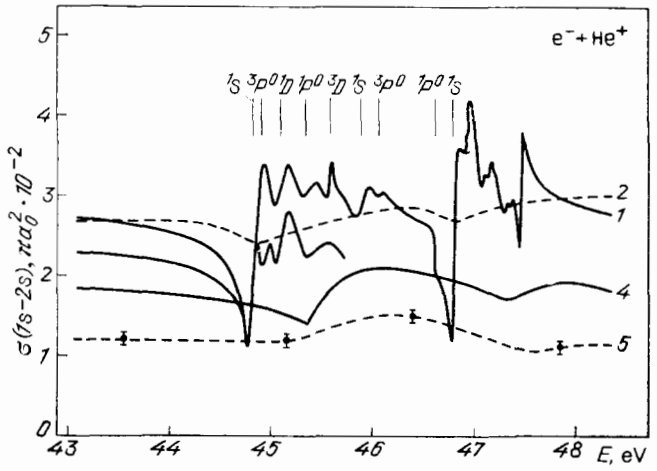


FIG. 8. Total cross section for electron-impact excitation of the 2s level of $He^+$. 1—Cross section found by the diagonalization method[26]; 2—cross section found by the diagonalization method and integrated with a Gaussian distribution function with a width of 1.5 eV (Ref. 26); 3—cross section calculated by the method of strong channel coupling with correlation functions[73]; 4—experimental cross section[68]; 5—experimental cross section.[75] The vertical lines mark the energy positions (3, $n\alpha$) of the autoionizing states of He.

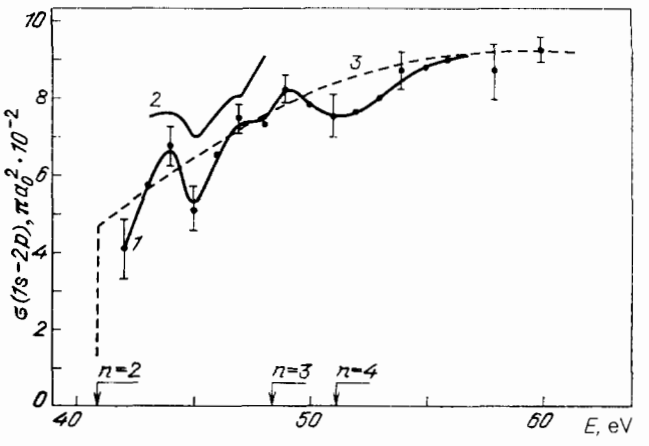


FIG. 9. Comparison of the average theoretical and experimental cross sections for electron-impact excitation of the 2p level of $He^+$. 1—Experimental cross section[72]; 2—cross section found by the diagonalization method and integrated with a Gaussian distribution function of width 1.5 eV (Ref. 26); 3—experimental cross section.[72]

pling with 20 states and pseudostates of $He^+$ was used to calculate the parameters of the autoionizing states of He below the $n = 2$ threshold of $He^+$. It was shown there that in the nonresonance energy region short-range electron-electron correlations are dominant, while in the region of resonances the long-range correlations are more important.

In concluding this section of the review we wish to stress that a detailed comparison of the resonance structure which has been calculated to date in the excitation cross section for the $n = 2$ levels of $He^+$, on the one hand, with experimental data on the other, will require experiments in which the energy spread of the electron beam is at most 0.1–0.2 eV. Achieving this figure seems totally realistic in view of the substantial progress which has recently been achieved in the experimental apparatus. Furthermore, if reliable experimental results are to be obtained it will be necessary to solve the problem of measuring absolute cross sections, since so far absolute cross sections have been found through the use of a procedure of normalizing the experimental curve to the Born-approximation theoretical curve in the region 100–300 eV. That method is not always justified.

## 7. ALKALI METAL ATOMS

A distinctive feature of the scattering of slow electrons by alkali atoms is the presence of a clearly expressed $^3P$ shape resonance in the elastic cross section. This resonance was originally predicted in theoretical calculations carried out by the method of strong coupling of $ns$-$np$ states by Karule.[77] The existence of a $^3P$ resonance was subsequently confirmed in other theoretical calculations.[78–80] Experimentally, the $^3P$ resonance has been observed by Jonston and Burrow[81] and Saelee and Lukas.[82] Table III shows the results of theoretical and experimental studies of the positions of the $^3P$ shape resonance. The shape resonances in the elastic scattering of electrons by alkali atoms stand tens of times above the background value of the cross section. This circumstance causes changes in the thermal conductivity, the electrical conductivity and the viscosity of a weakly ionized plasma, since these properties are determined primarily by the interaction of slow electrons with the neutral component of the plasma.[83]

Analyzing the question of the existence of $^3P$ shape resonance in e + Cs scattering, Fabrikant[80] concluded that in place of this resonance there is a $^3P$ bound state of the negative $Cs^-$ ion with an affinity energy $\sim 0.027$ eV. However, a final resolution of this question must await calculations using more-accurate atomic wave functions, which yield an accurate value of the polarizability of the Cs atom.

Like the hydrogen atom, the atoms of all the alkali elements can capture an additional electron, forming a stable negative ion in the $^1S$ state with an affinity energy ranging from 0.61 eV for $Li^-$ to 0.47 eV for $Cs^-$. All the other states of negative ions of alkali elements which have been recognized to date are unstable; i.e., they are autoionizing states. All these states lie below various excited states of the corresponding atoms and are seen as resonances in the cross sections for elastic and inelastic scattering of electrons by the neutral atoms. Since the excited states of the alkali atoms are not degenerate in the orbital angular momentum of the valence electron, $l$—in contrast with the hydrogen atom—only a limited number of autoionizing states can lie under each threshold.

TABLE III. Energies (in electron folds) of the $^3P$ shape resonance in electron scattering by alkali metals.

| Element | Theoretical | | | Experimental | |
|---|---|---|---|---|---|
| | Ref. 78 | Ref. 92 | Ref. 79 | Ref. 81 | Ref. 82 |
| Li | 0,06 | | | | |
| Na | 0,10 | | | 0,08±0,02 | |
| K | 0,0024 | 0,02 | | | |
| Rb | | | | <0,05 | |
| Cs | | | 0,00075 | | 0,15—0,30 |

### 7.1. Lithium atom

Burke and Taylor[84] pointed out the existence of $^1D$ and $^1P$ autoionizing states of the $Li^-$ ion below the excitation threshold of the 2p $^2P$ state of Li. These autoionizing states were not found in the calculations of Ref. 85, carried out by the multiconfiguration Hartree-Fock method. Those calculations did, on the other hand, reveal three autoionizing states below the excitation threshold of the 3s $^2S$ state and four below the excitation threshold of the 3p $^2P$ state. Later, the same autoionizing states, with the same energies as in Ref. 85, were found in the calculations of Ref. 28, by the method of superposition of configurations. The widths of the autoionizing states below the excitation threshold of the 3s $^2S$ state were also calculated in Ref. 28. Furthermore, two autoionizing states were found below the 3p $^2P$ threshold, and four below the 3p $^2P$ threshold.

Figure 10 shows the scheme of autoionizing states of the $Li^-$ ion as calculated in Refs. 28, 84, 85, and 86.

The scattering of electrons by Li atoms has been the subject of several experimental and theoretical studies (e.g., Refs. 81, 82, and 87 on the experimental side and Refs. 77–79 and 84 on the theoretical side). However, the amount of information available on the scattering of electrons by the Li atom is far smaller than that available on other alkali metals. In particular, until very recently there had been no theoreti-

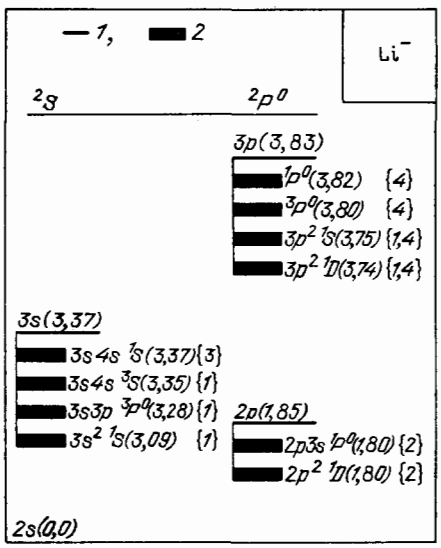


FIG. 10. Scheme of autoionizing states of the $Li^-$ ion. 1—Levels of Li; 2—levels of $Li^-$; 3—Ref. 28; 4—Ref. 84; 5—Ref. 86; 6—Ref. 85. The energies, in electron volts, are given in parenthesis.

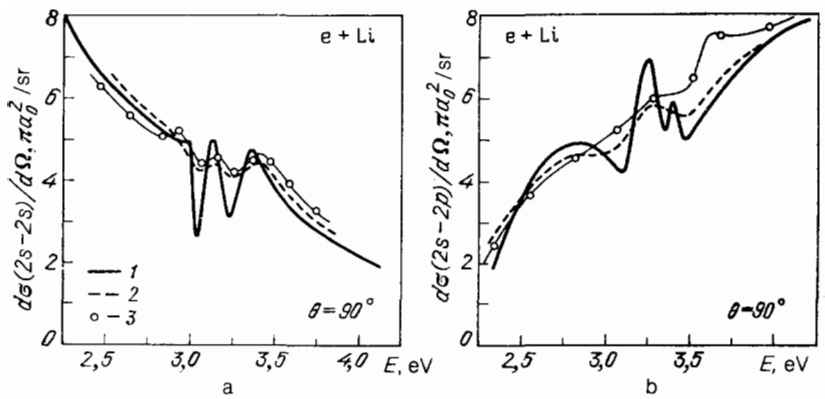


FIG. 11. Differential cross sections for (a) elastic e + Li scattering and (b) excitation of the 2p level at an angle of 90° as functions of energy.[28] 1—Calculated by the diagonalization method; 2—calculated by the diagonalization method and integrated with a Gaussian distribution function of width 0.3 eV; 3—experimental.

cal study of the formation of autoionizing states in experimental work on scattering, and the theoretical work has been restricted to the resonances in the elastic channel.[78,87]

Experimental and theoretical research was carried out[28] in 1984 on the differential cross sections for the elastic and inelastic scattering of electrons by the Li atom in the region above the 2p $^2$P excitation threshold. The differential cross sections for elastic scattering and excitation of the 2p $^2$P level through an angle of 90° were measured. The energy spread of the electron beam was 0.3 eV. The calculations were carried out by the diagonalization method, with allowance for two open channels. Resonances were seen quite clearly in the calculated partial cross sections. The contribution of resonances to the total and differential cross sections were less obvious. The reason was that the resonances were manifested in only the $^1$S, $^3$S, and $^3$P$^0$ waves, which correspond to partial cross sections which are small in comparison with those for the D, F, and G waves which dominate the cross section. Figure 11 shows results from Ref. 28. Since the magnitude of the differential cross sections was measured in arbitrary units, for comparison with the calculations the experimental curve has been shifted vertically to the extent which minimizes the discrepancy between the two curves far from resonances.

### 7.2. Sodium atom

Autoionizing states of $Na^-$ have been studied by the method of strong coupling of channels (Ref. 78, for example) and by the method of superposition of configurations.[85,88] Fung and Matese[85] have predicted $^1$P, $^1$D, and $^1$S autoionizing states with energies of 2 and 3.04 eV, respectively (the energies are reckoned from the ground state of the Na atom).

Figure 12 shows the results of some more comprehensive calculations which were carried out in Ref. 88. In that study, up to thirty Hartree-Fock configurations calculated with allowance for the polarization of the 2p$^6$ $^1$S core were chosen as a basis. The polarization of the core was taken into account by introducing a two-parameter potential in the Hamiltonian. The calculations revealed 28 autoionization states lying below the 6s threshold of the Na atom. Calculations were not carried out above this threshold. Among these autoionization states there are also three low-lying states, $^1$P, $^1$D, and $^1$S, which were predicted in Ref. 85. As we see from Fig. 12, several autoionization states with an identical term form below the 3d and 4d thresholds. This result is evidence that the Na atom has the strongest attractive potential in the excited $^2$D states.

Even P autoionization states and odd D autoionization states do not contribute to elastic scattering because of the conservation of parity and of the total orbital angular momentum (in the approximation of *LS* coupling). These states should be manifested in photoabsorption, superelastic scattering, and in excitation from the 3p level.

One of the earliest experiments on the scattering of electrons by the Na atom were those of Ref. 89, which was a study of the total cross section. In those experiments, however, an overly large energy step was chosen, and no resonant features of any sort were observed in the cross section. Kazakov *et al.*[90] have recently carried out a more accurate experiment, with an electron beam with an energy spread of 150 meV and with a small step along the energy scale. They determined the differential cross section for elastic scattering through an angle of 90°, and they found many structural features in the cross section. These results are compared in Fig. 13 with the results of calculations carried out by the

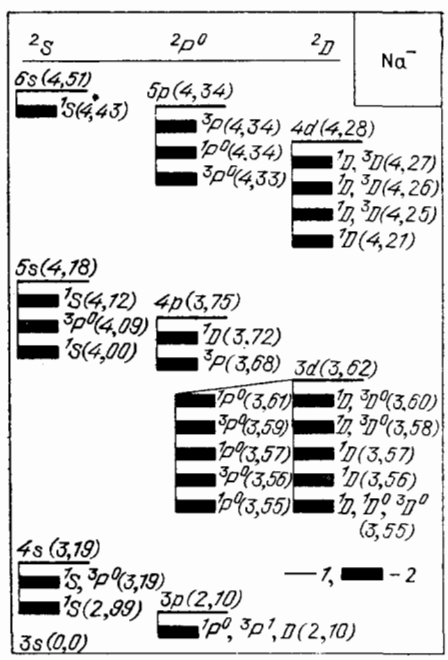


FIG. 12. Scheme of autoionizing states of the $Na^-$ ion.[88] 1—Levels of Na; 2—levels of $Na^-$. The energies, in electron volts, are given in parenthesis.

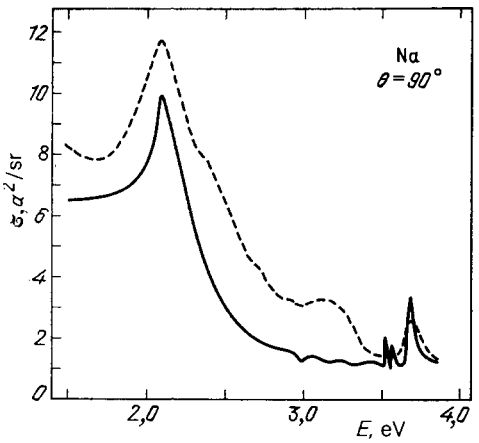


FIG. 13. Differential cross sections for elastic scattering of electrons by the Na atom.[90,91]

diagonalization method.[91] It can be seen from this figure that there are clearly expressed maxima in the cross section which correspond to $^1S$, $^{1,3}P^0$, and $^1D$ autoionization states, which lie below the 4s, 3d, and 4p thresholds. Near the excitation threshold of the 3p $^2P^0$ level of the Na atom, we see a structural feature in the cross sections which stems from the effect of the $^1P$ and $^1D$ autoionization states of the $Na^-$ ion and the opening up of a new channel in S-wave scattering. The effect of high-lying autoionization states on the total cross sections for elastic and inelastic scattering of electrons by Na atoms was studied theoretically in Ref. 88. The results are shown in Fig. 14. A comparison of Figs. 13 and 14 clearly demonstrates that a study of resonances through measurement of differential cross sections has advantages over measurements of total cross sections.

### 7.3. Potassium atom

Moores[92] has used the method of strong coupling in the approximation of 4s-4p-3d states to calculate the phase shifts in the elastic scattering of electrons by the K atom. It was found that the $^1P^0$ and $^3P^0$ phase shifts have a resonance behavior, which stems from the formation of an autoionization state of the $K^-$ ion below the excitation threshold of the 4p $^2P$ state. Greene's attempt[93] to confirm the existence of these autoionization states in calculations by a method of hyperspherical coordinates (more on this below) were unsuccessful. Lin[86] pointed out that the reason lay in the use in Ref. 93 of an overly crude approximation, specifically, the use of the Herman-Skillman potential to calculate the core field. The experiments of Ref. 94 reveal a resonant behavior of the differential scattering cross section between the thresholds of the excitation of the 4p and 5p levels. That behavior was attributed there to the formation during the scattering of intermediate autoionization states of the $K^-$ ion with total angular momenta $L = 0$, $L = 1$ (or $L = 3$), and $L = 2$ with energies of 2.4, 2.68, and 2.6 eV respectively. However, no theoretical description of these structural features in the cross section has yet been offered. Detailed data on the differential cross section for elastic scattering and excitation of the 4p level were reported in Ref. 90.

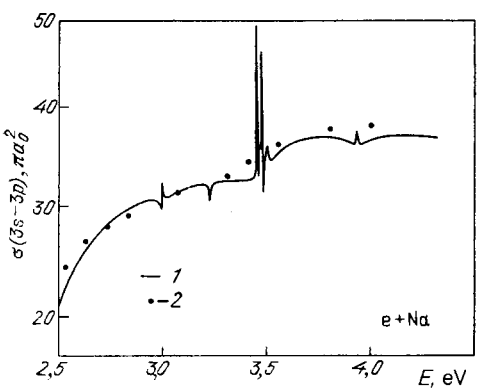


FIG. 14. Total cross section for electron-impact excitation of the 3p $^2P^0$ level on the Na atom. 1—Calculated by the diagonalization method[88]; 2—experimental.[36]

### 7.4. Cesium atom

The scattering of low-energy electrons by Cs atoms has been the subject of many studies (see, e.g., Refs. 95–98). As of yet, however, we have no results of a detailed experimental study of resonances in e + Cs scattering although such experiments are planned for the near future.[98] Our primary source of information of the autoionization states of the $Cs^-$ ion and their role in e + Cs scattering is thus the theoretical work. The most comprehensive calculations on resonances in e + Cs scattering were carried out by the $R$-matrix method with a spin-orbit interaction in Refs. 97 and 98. It was found that the cross sections have a complex structure near the 6p $^2P_{1/2,3/2}$ and 5d $^2D_{3/2,5/2}$ excitation thresholds. Figure 15 shows total cross sections for elastic scattering and for excitation of $^2P_{1/2,3/2}$ levels.

In order to detect and classify resonances, Scott *et al.*[98] carried out a detailed analysis of the energy dependence of the sum of intrinsic phase shifts (i.e., the phase shifts of the elements of the matrix found as a result of the diagonalization of the $S$ matrix) for each fixed value $J = 0, 1, 2, 3$, and 4 and for a fixed parity $\pi = \pm 1$. They found 25 resonances, to all of which except two they assigned a definite configuration (Table IV). In that table, each family of resonances

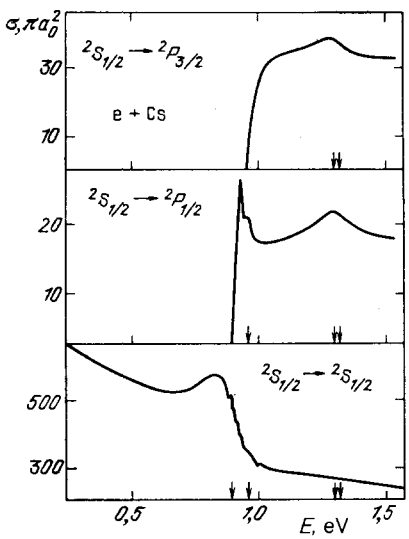


FIG. 15. Total scattering cross sections and cross sections for the electron-impact excitation of $^2P^0_{1/2,3/2}$ levels of Cs (Ref. 98). The arrows show the $^2P_{1/2}$, $^2P_{3/2}$, $^2D_{3/2}$, and $^2D_{5/2}$ thresholds of Cs.

TABLE IV. Configurations of resonances observed in e + Cs scattering.[98]

| | | | |
|---|---|---|---|
| A | $6pns\ ^3P_{0,1,2}$ | G | $6p5d_k^1D_{1,2,3}$ |
| B | $6p5d\ ^3D_{1,2,3}$ | H | $6p^2\ ^1S_0$ |
| C | $6s6p\ ^1P_1$ | I | $6p^2\ ^3P_{0,1,2}$ |
| D | $6p5d\ ^3F_{2,3,4}$ | J | $6s5d\ ^3D_{1,2,3}$ |
| E | $6p5d\ ^1D_2$ | K | $6pnp\ ^3D_{1,2,3}$ |
| F | $6p5d\ ^1F_3$ | | |

which have the same configuration, orbital angular momentum, and spin and which lie below the same threshold are denoted by a capital letter.

Among the resonances distinguished there are also some (A and K in Table IV) which stem from the capture of the impinging electron at a large distance by the long-range potential of the excited Cs atom. We should emphasize, however, that the classification of resonances on the basis of the definite configurations assigned to them is extremely approximate because of the strong interconfigurational interaction. With regard to the positions of these resonances, we note that the A, D, H, and I resonances lie directly below the $^2P_{1/2}$ threshold; C, E, and K lie between the $^2P_{1/2}$ and $^2P_{3/2}$ thresholds, B and F lie between the $^2P_{3/2}$ and $^2D_{3/2}$ thresholds; and G lies between the $^2D_{3/2}$ and $^2D_{5/2}$ thresholds. The resonances are less obvious in the cross sections, because a large number of resonances differing in symmetry overlap along the energy scale and interfere strongly in the total cross section. We can offer a few generalizing comments regarding the role played by electron-electron correlations in the formation of autoionization states of negative ions of alkali atoms.

The model of independent electrons is applicable in most cases for describing singly excited states of atoms. In this model it is assumed that each electron is moving in the field of the nucleus and of the other electrons and has its own wave function. Each state of the atom is characterized by a definite configuration. This model, however, gives a poor description of the autoionization states of atoms. It has proved to be a particularly unsound choice in attempts to describe the autoionization states of negative ions, since electron-electron correlations play an even greater role in this case.

All the calculations which have been carried out on the autoionization states of the ions of alkali atoms indicate a strong configurational mixing. The nature of this mixing is such that one can distinguish two extreme methods for the formation of autoionization states.[99,100] In one case, the excited atomic electron and the captured electron form a highly correlated pair and move at approximately the same distance from the nucleus. The radial correlation in the motion of electrons is important here. In the second case, the impinging electron is captured at a great distance. The average distances from the electrons to the nucleus are quite different in this case, and there is a pronounced angular correlation in their motion. Correlations in the motion of two excited electrons were analyzed in much detail in an excellent review by Fano.[100]

The most popular methods for calculating the parameters of the autoionization states of negative ions are the Hartree-Fock multiconfiguration method and the method of superpositions of configurations. These methods, however, do not generate anything in the way of a natural classification of autoionization states. For this reason, considerable interest has been attracted to the method of hyperspherical coordinates,[100,101-105] in which the wave function of the two electrons is written as an expansion in the eigenfunctions of the "angular momentum" operator in a six-dimensional space. This method not only allows a systematic description of the parameters but also generates a natural classification of autoionization states. On the other hand, this method is rather complicated and has accordingly been used in only a comparatively few calculations so far.

At present we have far more theoretical than experimental information on resonances in the collisions of electrons with alkali atoms. As we have seen, in the case of light alkali atoms the resonances lie nearly at the thresholds and lie very close to each other. High-resolution apparatus is accordingly required to observe them. Since the resonances are seen far more clearly in the differential cross sections than in the total cross sections for the cases of Li, Na, and K atoms, we need more experimental data on the differential cross sections, especially on their absolute values in order to observe and reliably identify these resonances. It would also be extremely valuable to have results obtained from experiments with polarized (see Sec. 10) monoenergetic beams of electrons and alkali atoms at energies in the resonance region. On the theoretical side, we need further and more accurate calculations of the parameters of the resonances, incorporating electron-electron correlations at a very high accuracy. We also need new methods for calculating cross sections for excitation from excited levels.

## 8. IONS OF ALKALI AND ALKALINE EARTH ELEMENTS

The reason for the interest in the ions of alkaline earth elements is that processes involving these ions play an exceedingly important role in astrophysical and fusion research, in experiments in the space environment of the earth, in laser technology, and in other promising scientific and technological directions. For example, back in the early 1960s astrophysical studies of the solar chromosphere established[106] that the power of the radiation from the chromosphere at the wavelength $\lambda = 2800$ Å, which corresponds to the transition $3s\ ^2S_{1/2} - 3p\ ^2P_{1/2,3/2}$ $Mg^+$, occupies second place after the radiation in the $L_\alpha$ lines of atomic hydrogen. The radiation from ionized calcium and barium is also known to be important in astrophysics. In particular, resonance K and H lines of $Ca^+$ are exceedingly important sources of information about the solar chromosphere.

A promising direction for pulsed gas lasers is to make use of the lasing action of self-limiting transitions of $Ca^+$ and $Ba^+$ ions[110] and also of the afterglow of discharges involving transitions of $Mg^+$, $Ca^+$, $Sr^+$ and $Ba^+$ (Ref. 111). The role played by resonances can be expected to be far more significant in the scattering of electrons by ions than in the scattering of electrons by atoms. The reason is that, as was shown by Presnyakov[112], there is an infinite series of resonances below each excitation threshold of the ion, in contrast with the situation in the case of atoms. Furthermore, this role should increase in importance with increasing charge of the ion.[113] Some new experiments have recently been carried out on the cross sections for the excitation of $Mg^+$ and $Sr^+$ by low-energy electrons.[114,115] These experiments have yielded

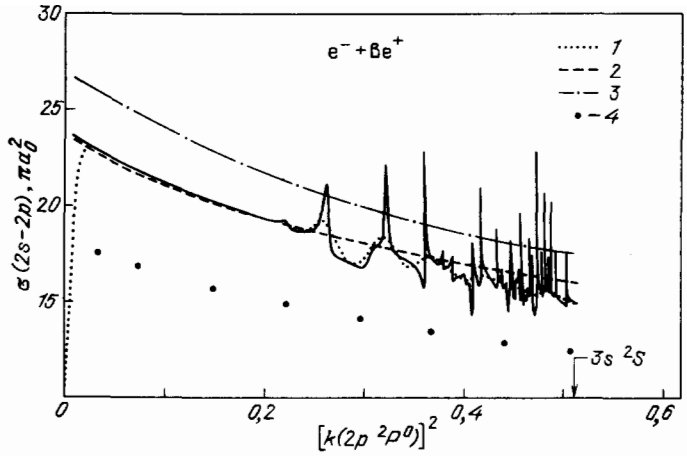


FIG. 16. Total cross section for electron-impact excitation of the 2p $^2P^0$ level of $Be^+$ (Ref. 117). 1—Cross section found by a diagonalization method and integrated with a Gaussian distribution with a width of 0.3 eV (Ref. 117); 2—cross section found by the method of strong coupling with allowance for the 2s and 2p states of $Be^+$ (Ref. 118); 3—cross section found in the Coulomb-Born approximation[118]; 4—experimental cross section.[116]

the first observation of a clearly defined resonance structure in these cross sections.

Since we do not yet have any experimental data on the cross sections for the elastic scattering of electrons by the ions of alkaline earths let us examine experiments on the excitation of these ions by electrons. There have been extremely few studies of the resonance structure in the cross section for the excitation of ions by electrons.

For the $Be^+$ ion, we have only the single experiment which was carried out by Dunn's group,[116] who studied the excitation cross section of the 2p $^2P^0$ resonance level; however, no resonance structure was found in the cross section near the threshold (Fig. 16).

A first experiment on the excitation of the 3p $^2P^0$ resonance level of the $Mg^+$ ion has been carried out at Uzhgorod State University.[119] The excitation cross section of the resonance level of the $Mg^+$ ion was measured at energies ranging from the excitation threshold up to 100 eV. A significant structure was observed near the threshold; Kel'man *et al.*[119] originally attributed this structure to effects of a cascade filling of an $Mg^+$ resonance level. Recently, the same investigators used an optical method to carry out some more careful experiments on the excitation by electrons of the $3p^2\ P^0$ level of $Mg^+$ (Ref. 114), with an electron beam with a much smaller energy spread ($\sim 0.3$ eV as against the $\sim 1$ eV in Ref. 119). As a result, a very clearly defined resonance structure was found in the excitation cross section; this structure was attributed to effects of capture of electrons into autoionization states of Mg (Fig. 17).

The same group has carried out studies of resonances in the cross sections for the excitation for the $np^2P^0$ levels of the ions $Ca^+$ ($n = 4$; Ref. 120), $Sr^+$ ($n = 5$; Ref. 115), and $Ba^+$ ($n = 6$; Ref. 121) with an electron beam with an energy spread of 0.2 eV. Since the fine splitting of the $^2P$ levels in the ions of heavy alkaline earth elements reaches a significant magnitude ($\sim 0.028$ eV for $Ca^+$, $\sim 0.099$ eV for $Sr^+$ and 0.210 eV for $Ba^+$), it turned out to be possible to study separately the resonance structure in the excitation cross sections of the sublevels with $j = 1/2$ and $j = 3/2$. The results of these experiments for the $Ba^+$ ion are shown in Fig. 18.

The measured excitation cross sections typically reveal the following behavior: a fast increase in the cross section at the threshold, the presence of structural features consisting of several maxima, a sharp decay of the cross section by a factor of two or three in the interval between 6 eV and the ionization potential, and the decay $\sigma \sim E^{-1}$ at large energies.

Turning to theoretical calculations of resonances in the cross sections for the scattering of electrons by the ions of alkaline earth elements, we note that so far such calculations have been carried out for only the differential cross sections for the elastic scattering $e^- + Be^+$ and $e^- + Mg^+$ (by the diagonalization method[27]) and the excitation cross sections

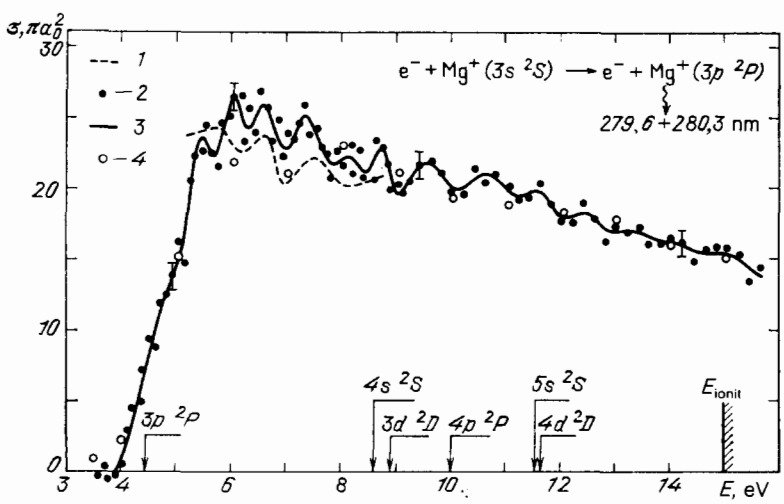


FIG. 17. Total cross section for electron-impact excitation of the 3p $^2P^0$ level of $Mg^+$. 1—Cross section found by the diagonalization method and integrated with a Gaussian distribution with a width of 0.3 eV (Ref. 114); 2—experimental cross section[114]; 3—analysis of the experimental results of Ref. 114 by a digital filtering method; 4—experimental cross section.[119]

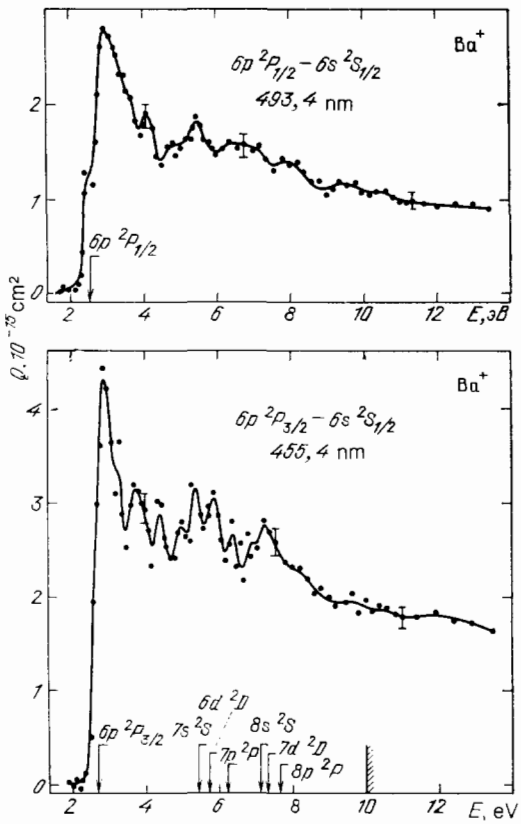


FIG. 18. Total cross section for electron-impact excitation of the components of the $6p\ ^2P^0_{1/2,3/2}$ level of $Ba^+$ (Ref. 121).

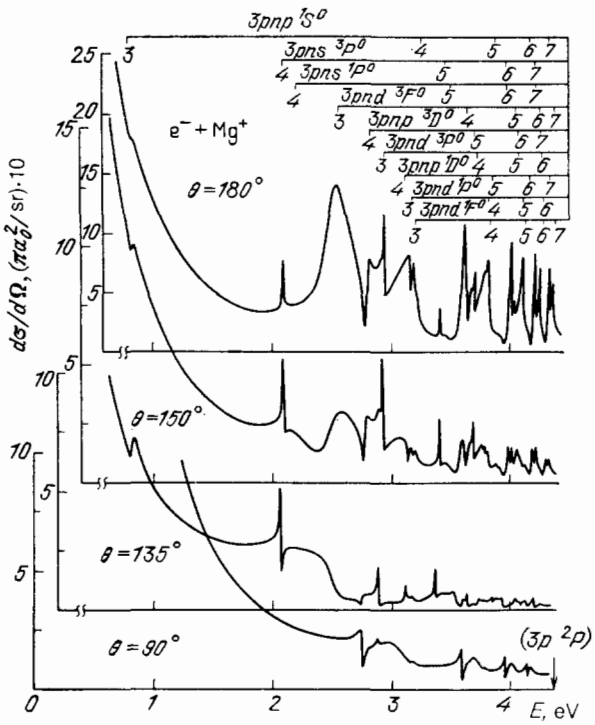


FIG. 19. Energy dependence of the differential cross section for elastic scattering of electrons by the $Mg^+$ ion for various scattering angles.[27]

of the $2p\ ^2P^0$ level of $Be^+$ (by the diagonalization method) and the $3p\ ^2P^0$ level of $Mg^+$ (by the method of strong coupling[123] and by the diagonalization method[117]). No calculations of any sort have been carried out on the resonances in the excitation cross sections of the $Ca^+$, $Sr^+$, and $Ba^+$ ions.

In Ref. 27 we studied the energy dependence of the differential cross section for the elastic scattering $e^- + Be^+$ for various scattering angles; we also found the positions of resonances with $\Gamma > 10^{-4}$. The results established that the resonances are manifested most clearly in the scattering through large angles. In contrast with the cross section for photoionization of Be from the ground state, where all the structure is determined (entirely) by the broad $2pns\ ^1P^0$ resonances and the narrow $2pnd\ ^1P^0$ resonances, the structure in the cross section for the elastic scattering $e^- + Be^+$ is dominated by the triplet resonances $2pnd\ ^3P^0$, $2pnp\ ^3D$ and $2pnd\ ^3F^0$ and the singlet $2pnd\ ^1F^0$ resonances. The singlet S, P, and D resonances, on the other hand, make a significantly smaller contribution. At the scattering angle $\theta = 180°$, the $^{1,3}F^0$ resonances give rise to a series of clearly defined peaks in the cross section; against the background of these peaks, the $2pnd\ ^3P^0$ and $2pnp\ ^3D$ resonances are seen as narrow minima.

The resonance structure in the differential cross section for the elastic scattering of electrons by the $Be^+$ ion is significantly richer and qualitatively different from the structure of the corresponding cross section for the $He^+$ ion. The reason is that the widths of the $2pnl$ autoionization states of Be are, on the whole, substantially greater than the widths of the $(2n, \alpha)$ autoionization states of He. While the widths of the $2pnd\ ^3P^0$ autoionization states of Be for $L = 1$ are only twice as great as the widths of the $2pns\ ^3P^0$ autoionization states of He, for $L = 2$ the values of the widths of the $2pnp\ ^3D$ autoionization states of Be are more than an order of magnitude greater than the width of the $(2n, \alpha)\ ^3D$ autoionization states of He. For the autoionization states with $L = 3$, which determine the behavior of the cross section for the elastic scattering of electrons by $Be^+$, this difference increases to two orders of magnitude.

Figure 19 shows the energy dependence of the differential cross section for the elastic scattering of electrons by the $Mg^+$ ion; the positions and configurations of the corresponding autoionization states of Mg are also shown here. We see that again the structure in the cross section is determined primarily by triplet resonances; seen particularly clearly is a low-lying $3p3d\ ^3F^0$ resonance with a width $\Gamma = 0.264$ eV.

As for the very broad $3pns\ ^1P^0$ resonances, which completely determine the shape of the cross section for photoionization of Mg from the ground state at energies in the threshold region, we note that their contribution to the elastic cross section can be detected only at angles $\theta = 135°$, where the peaks due to the $^{1,3}F^0$ resonances disappear almost entirely. At these scattering angles, the low-lying $3p4s\ ^1P^0$ resonance ($\Gamma = 0.585$ eV) is seen as a very rounded maximum near 2 eV.

The absence of any other (theoretical or experimental) results on the differential cross sections for elastic scattering of electrons by $Be^+$ and $Mg^+$ ions rules out a comparative analysis of the theoretical data obtained by the diagonalization method and reported above. It would be extremely useful to see an experiment on these processes, since the resonance structure predicted theoretically in the elastic cross sections is very vivid (particularly in the case of the $Mg^+$ ion) and can be detected by the method of intersecting elec-

tron and ion beams with existing experimental apparatus.

Figure 16 shows the results of calculations of the total cross section for excitation of the resonance level of $Be^+$ along with some experimental results.[116] As expected, far from the resonances ($k^2 \leqslant 0.2$ Ry) the cross section calculated by the diagonalization method agrees with the cross section found in Ref. 118 by the method of strong coupling of 2s-2p states of $Be^+$. In the resonance region the cross section exhibits a significant structure, due for the most part to triplet resonances with $L > 1$. As the energy is raised ($k_2^2 > 0.4$ Ry), the resonances become more closely spaced and are seen as a continuous network of very narrow peaks in the cross section, rising by $(3–5)\pi a_0^2$ above the general value of the cross section.

To evaluate the effect of resonances on the excitation cross section under the conditions of an actual experiment, the theoretical cross section was averaged over the energy distribution of the beam electrons with a width of 0.3 eV.

Figure 17 shows the results of calculations by the diagonalization method on the excitation of a resonance level of $Mg^+$, along with the results of a recent experiment by Zapesochnyĭ *et al.*[114] It can be seen from Fig. 17 that the cross section calculated by the diagonalization method, and averaged in accordance with the experimental conditions, agrees very well in both magnitude and shape with the experimental cross section found through an additional processing of the measured results by digital filtering methods. The experimental cross section does exceed the calculated cross section somewhat ($\sim 6\%$), apparently because of an imperfect procedure for normalizing the experimental cross section to the theoretical cross section found in the Coulomb-Born approximation at 100 eV.

Figure 20 compares the cross section calculated by the diagonalization method with results of some other theoretical calculations. We see that the resonance structure found in the excitation cross section by the strong-coupling method in Ref. 122 correlates well with the shape of the resonances calculated by the diagonalization method. However, despite the fact that the relative positions of the resonance features on the curves agree very well with each other, on the curve found by the strong-coupling method these features are shifted about 0.25 eV up the energy scale. This shift of the Mg resonances to higher energies occurs because Ref. 122 ignored some of the correlations which give rise to the dipole polarizability of the 4s $^2$S state of $Mg^+$. In the calculations by the diagonalization method, the dipole polarizability was taken into account by incorporating 4p$n$ (s,d) configurations in the basis. It can be seen from Fig. 17 that this approach leads to a very good agreement between the resonance structure observed experimentally in the excitation cross section of the 3p $^2$P$^0$ level of $Mg^+$ and that found in calculations by the diagonalization method.[114]

We turn now to a brief assessment of the situation regarding ions of alkali elements. Some extremely interesting results on the electron-impact excitation of ions of alkali elements were recently obtained.[124] A first study has been made of the emission accompanying inelastic collisions of $K^+$, $Rb^+$, and $Cs^+$ ions with electrons over the energy range 8–400 eV. The clearly expressed structure found here indicates that the interaction is of a resonance nature. Zapesochnyĭ *et al.*[124] suggest that the decay of certain autoionization states to the resonance level of the ion occurs without a change in the quantum numbers $n_{1+}$, $l_1$ of the excited electron (a Coster-Kronig process):

$$A^+(np^6) + e \to A^{**}[np^5(^2P_{1/2})\, n_1 l_1 n_2 l_2]$$
$$\to A^{+*}[np^5(^2P_{3/2})\, n_1 l_1] + e.$$

As the resonance level of the ion goes lower, the resonance structure in the excitation cross section of this level typically becomes richer. A similar situation has been observed[125] in the case of the excitation of the $Tl^+$ ion by electrons. Unfortunately, we do not yet have any theoretical calculations which would confirm or refute these comments regarding alkali element ions.

In summary, the situation regarding research on resonances in electron-ion collisions is less favorable than the situation regarding research on the scattering of electrons by atoms. The experimental information is scanty. The complete absence of experimental data on differential cross sections hinders a classification of the resonances in several cases. The large energy spread of the electron beam has made it impossible to compare theory and experiment in detail.

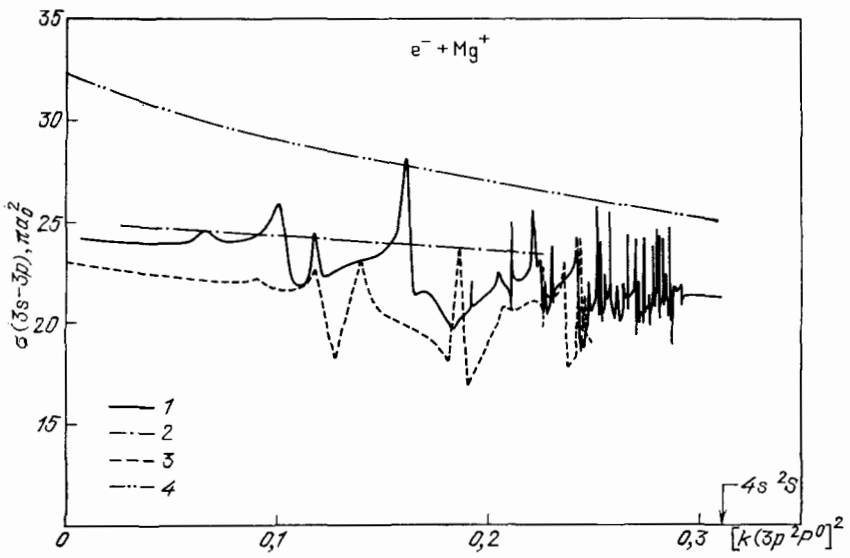


FIG. 20. Comparison of results of calculations of the total cross section for electron-impact excitation of the 3p $^2$P$^0$ level of $Mg^+$. 1—Cross section found by the diagonalization method[114]; 2—by the method of strong coupling of three states (3s-3p-3d) of $Mg^+$ (Ref. 123); 3—by the method of strong coupling of four states (3s-3p-4s-3d) of $Mg^+$ (Ref. 122); 4—by the Coulomb-Born approximation.[172] Here $[k(3p\ ^2P^0)]^2$ is the energy of the electrons in the excitation channel of the 3p$^2$P$^0$ level of $Mg^+$ (in rydberg).

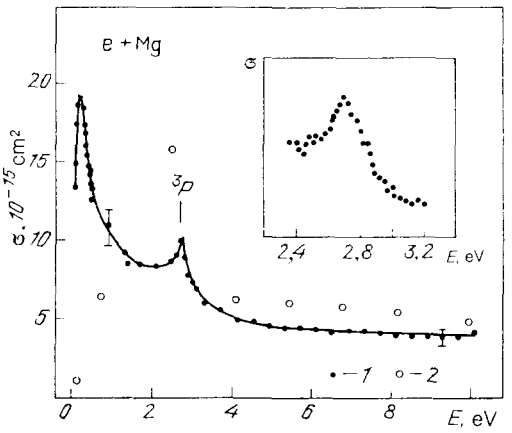


FIG. 21. Total cross section for electron scattering by Mg atoms. 1—Experimental results of Ref. 128; 2—theoretical results of Ref. 130.

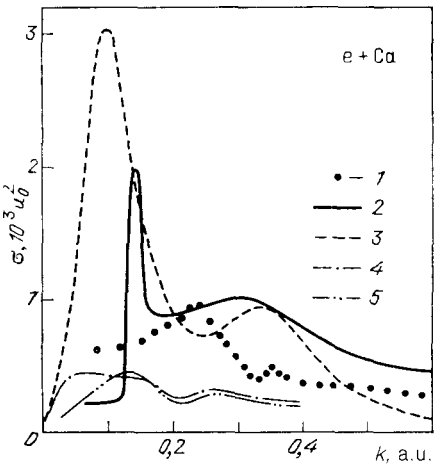


FIG. 22. Total cross section for the elastic scattering of slow electrons by the Ca atom. 1—Experimental[11]; 2—calculated in the random phase approximation with exchange[131]; 3—calculated by a simplified version of the random phase approximation with exchange[131]; 4—calculated by the method of strong coupling of $4^1S$-$4^1P$-$4^3P$ states of Ca (Ref. 130); 5—calculated by the method of strong coupling of $4^1S$-$4^1P$ states of Ca (Ref. 130).

## 9. GROUP II ATOMS

Since the two valence electrons of the group II atoms in the periodic table form an $ns^2$ subshell, these atoms do not have stable negative ions, in contrast with alkali atoms. When electrons are scattered by these atoms, however, unstable states of negative ions may form; the decay of these states is manifested as structural features in both the scattering cross sections and the optical excitation functions. Indeed, such structural features have been found in many theoretical and experimental studies.

We begin with the shape resonances which are observed in the cross sections for the elastic scattering of electrons by group II atoms.

The transmission experiment of Ref. 126 revealed $^2P$ shape resonances in the elastic scattering of electrons by Mg, Cd, Zn, and Hg atoms. In some more recent experiments[11,127] carried out by the method of intersecting atomic and electron beams, with detection of the scattered electrons, the total cross sections for the scattering of electrons by Mg, Ca, Sr, and Ba atoms were measured over the energy interval 0–10 eV. These experiments confirmed the existence of a $^2P$ resonance in e + Mg scattering (Fig. 21) and revealed $^2D$ shape resonances in the elastic scattering of electrons by Ca, Sr, and Ba atoms.

The existence of $^2P$ shape resonances in the elastic scattering of electrons by the Be and Mg atoms has been predicted in many places (see, e.g., Refs. 129 and 130). Kurtz and Ohrn[129] solved the scattering problem in the one-channel approximation with a potential $V = V_s + V_{pol}$ where $V_s$ is the static potential of the atom, while $V_{pol}$ is a phenomenological polarization potential. Fabrikant[130] calculated the cross sections for elastic e + Be and e + Mg scattering in the approximation of strong coupling of three states: $n^1S$, $n^1P$, and $n^3P$ ($n = 3, 4$ for Be and Mg, respectively). The $^2P$ resonance was found in Fabrikant's calculations[130] only for e + Be scattering. A possible reason for the absence of a resonance in the calculations of Ref. 130 for the Mg atom is an insufficiently small energy step in those calculations.

Calculations have been carried out on elastic e + Ca scattering by the method of strong coupling of two and three states[130] and in the random phase approximation with exchange.[131] The results found in Ref. 131 indicate the existence of two maxima (Fig. 22), which the authors interpret as shape resonances. The first maximum, formed by a p wave at an energy of 0.27 eV, was not found in the experiments of Ref. 11. The second maximum is formed primarily by the d wave and lies at an energy ~1.35 eV. The experiments of Ref. 11 revealed two $^2D$ resonances in the elastic cross section, but the first resonance, a shape resonance, occurred at a far lower energy, ~0.7 eV, while the second, which appeared at ~1.7 eV, was classified by Romanyuk *et al.*[11] as a Feshbach resonance. In the calculations of Ref. 130, on the other hand, there was no P resonance at all near the elastic threshold. Amus'ya *et al.*[131] explained this fact by arguing that the calculations of Ref. 130 were carried out with crude semiphenomenological wave functions for the Ca atom.

Fabrikant[130] carried out a theoretical study of e + Sr and e + Ba scattering by the method of strong coupling of two and three states. Those calculations rvealed a $^2D$ shape resonance in elastic e + Sr scattering which had been observed in the experiments of Ref. 11. However, those calculations did not reveal the $^2D$ shape resonance in elastic e + Ba scattering which had also been observed in Ref. 11. A possible reason is that, as in the case of e + Mg scattering, the step along the energy scale was chosen insufficiently small in those calculations.

Table V shows the positions and widths of the shape resonances in the elastic scattering of electrons by these group II atoms.

We turn now to the Feshbach resonances which have

TABLE V. Energies and widths of shape resonances in the elastic scattering of electrons by group II atoms.

| | $E$, eV | $\Gamma$, eV |
|---|---|---|
| Mg | 0.15 | 0.14 |
| Cd | 0.33 | 0.33 |
| Zn | 0.49 | 0.45 |
| Hg | 0.63 | 0.4 |

been observed in collisions of electrons with group II atoms.

A resonance below the excitation threshold of the $3^3P$ level of the Mg atom, at an energy of 2.7 eV, was first observed in the experiments of Ref. 10. Burrow and Comer[10] believed that this resonance was due to the $3s3p^2\ ^2D$ state of the $Mg^-$ ion, and they linked it with a D resonance which had been calculated theoretically in Ref. 130 and which lay at an energy of 2.6 eV. The same resonance has been observed in the experiments of Ref. 127 and 128, which we have already mentioned, at an energy of 2.7 eV (Fig. 22). Romanyuk *et al.*[11] also observed resonances below the first excitation threshold in electron scattering by Ca and Sr atoms (Fig. 22). Although no resonances were seen experimentally under the first excitation threshold of the Ba atom, the calculations of Ref. 130 clearly reveal a rather broad maximum in the partial cross section $\sigma(L = 1)$ at an energy $\sim 2.04$ eV. Many resonances were observed in the excitation cross sections of levels of the Mg atom in Ref. 132 in measurements of optical excitation functions.

The first study of resonances in the excitation cross sections of Zn and Cd atoms was carried out by Shpenik *et al.*, who used an optical method.[7,133] In the $5\ ^3S_0$ and $6\ ^3S_1$ optical excitation functions of the Zn and Cd atoms, respectively, measured with a very small energy spread, $\Delta E \sim 80$ meV, several structural features were observed; after the contribution of cascade transitions was separated out, it was found possible to interpret those features as Feshbach resonances.

Table VI summarizes the experimental and theoretical results on the positions and classification of the resonances in the elastic-scattering cross sections (except shape resonances) and in the excitation cross sections for Ca, Sr, Ba, Mg, Zn, and Cd atoms.

Resonances in the excitation cross sections of Hg atoms have been studied in great detail.

The first hints of their existence appeared in studies by Shpenik *et al.*[7,133] as early as 1965. Figure 23 illustrates the results with the excitation functions which they found for the lines of the mercury atom at $\lambda = 5461$ Å ($6\ ^3P_2 - 7\ ^3S_1$) and $\lambda = 2537$ Å ($6\ ^1S_0 - 6\ ^3P_1$).

Also in 1965, Kuyatt *et al.*[5] reported the observation of thirteen structural features in the energy dependence of the current of electrons passed through mercury vapor. An analysis carried out by Fano and Cooper[134] made it possible to interpret some of these structural features, as originating from the formation of short-lived states of the $Hq^-$ ion. Ottley and Kleinpoppen[135] subsequently measured the optical excitation function of an intercombinational line of mercury and its polarization. The results of Ref. 135 agree well with the results of a high-precision study[12] of optical excitation functions (with a resolution $\sim 0.04$ meV). Fifteen resonances were found between 4.5 and 12.5 eV in that study.

Resonances in e + Hg scattering have since then been the subject of many studies. Newman *et al.*[136] recently carried out some extremely high-precision measurements of the excitation cross section of metastable levels of Hg, with an energy resolution of 25 meV. They observed a rich resonance structure between 8.5 and 11 eV.

TABLE VI. Energies (in electron volts) and classification of resonances in the elastic scattering cross sections and excitation cross sections of group II atoms.

| Atom | Experiment | Theory | Configuration, term |
|---|---|---|---|
| Ca | 1,7±0,1[132] | 1,77[130] | $3d^24s$ or $3d4s4p$ P |
| Sr | 1,2±0,1[132] | 0,95[130] | $4d^25s$ or $4d5s5p$ D |
| Ba | 3,92 [132] | | 5s5p6s P |
| Mg | 2,7±0,3[132]<br>3,1 [132]<br>4,4 [132]<br>4,7 [132]<br>5,2 [132]<br>5,7 [132]<br>6,3 [132]<br>6,5 [132]<br>6,7 [132]<br>7,0 [132]<br>7,4 [132] | 2,58[130] | $3s3p^2$ D<br>$3s^23d\ ^2D$<br>$3s^24p\ ^2P^0$<br>$3s3p^2\ ^2S$<br>$3s3p^2\ ^2P$<br>$3s3p4s\ ^4P^0$<br>$3s3p3d\ ^2D^0$<br>$3s3p3d\ ^2P^0$<br>$3s3p5s\ ^2P^0$<br>$3s3p4d\ ^2P^0$<br>$3s3p5d\ ^2P^0$ |
| Zn | 7,18 [133]<br>7,56 [133] | | |
| Cd | 6,75 [133]<br>7,24 [133] | | |

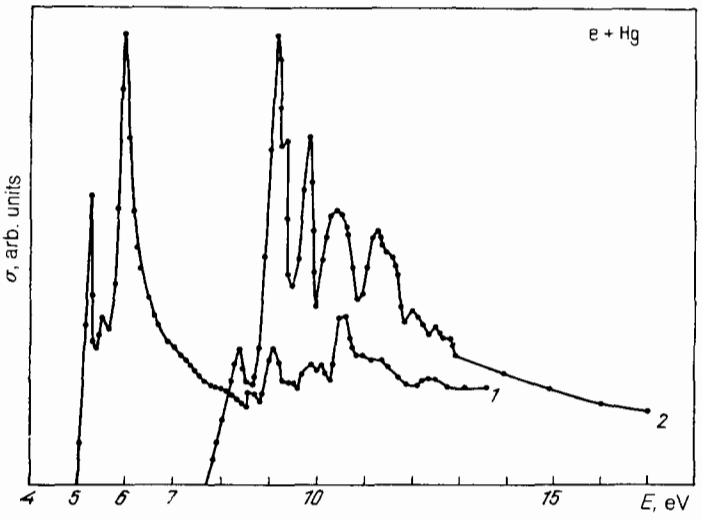


FIG. 23. Energy dependence of the excitation cross sections of lines of the mercury atom.[7] 1—$\lambda = 2537$ Å ($6\ ^1S_0 - 6\ ^3P_1$); 2—$\lambda = 5461$ Å ($6\ ^3P_2 - 7\ ^3S_1$).

TABLE VII. Energies and classification of resonances in e + Hg scattering. The energies are given in electron volts.

| Classification[141,145] | Ref. 5 | Ref. 126 | Ref. 12 | Ref. 135 | Ref. 137 | Ref. 140 |
|---|---|---|---|---|---|---|
| $6s^26p\ ^2P$ | | 0,63 | | | | |
| $6s6p^2\ ^4P_{1/2}$ | 4,07 | | | | 4,55 | 4,7 |
| $6s6p^2\ ^4P_{3/2}$ | 4,30 | | 4,70 | | 4,71 | 4,7 |
| $6s6p^2\ ^4P_{5/2}$ | 4,89 | | 4,90 | 4,92 | 4,94 | 4,9 |
| $6s6p^2\ ^2D_{3/2}$ | | | | 5,23 | | 5,5 |
| $6s6p^2\ ^2D_{5/2}$ | | | | 5,50 | 5,51 | 5,5 |

Albert *et al.*[137] have measured the differential cross sections for elastic scattering over the interval 4.5–6 eV. These measurements and also the theoretical analysis of all the results on resonances which was carried out by Heddle[138] provide a reliable classification of the resonances in this energy region.

Kazakov *et al.*[139] also measured the differential cross sections for elastic and inelastic scattering of electrons by Hg atoms through an angle of 90°. Their results on the elastic scattering support the data found in earlier studies.

The most comprehensive theoretical interpretation of elastic e + Hg scattering and of the excitation of the 6s6p $^3P_{0,1,2}$ and 6s6p $^1P_1$ states was generated by Burke *et al.*[140] who used a $R$-matrix method and considered five states at energies near the threshold. As can be seen from Table VII, the theoretical results of Ref. 140 agree extremely well with the experimental data of Refs. 12, 135, and 137.

Recent improvements in experimental apparatus have made it possible to observe the excitation of excited atoms by electrons (stepwise excitation). Gallagher[36] recently carried out an experiment on the excitation of the Na atom from the 3p level. An extensive research program has been carried out by Aleksakhin *et al.*[141,142] on the excitation of Na*, Ca*, Ba*, and Sr*. Interestingly, the cross sections for stepwise excitation are significantly larger—by a factor of hundreds in some cases—than the cross sections for the excitation of the same levels from the ground state. A significant maximum becomes very distinct near the threshold; it may be a shape resonance. As yet, we have no theoretical interpretation of these results.

## 10. POLARIZATION EFFECTS IN SCATTERING

Polarization experiments are extremely important for reaching a deeper understanding of collision processes in atomic physics. Progress in the development of sources of polarized electrons and of intense atomic beams polarized by laser radiation has provided a new impetus to research on spin-dependent effects in electron-atom collisions.

We recall that the primary quantities in the theory are amplitudes which depend, at a given energy, on the projections of the spins of the impinging electron and of the atomic target in the initial and final states. The total cross section is found by integrating over angles, summing over the projections of the final-state spins, and averaging over the projections of the initial-state spins. Consequently, measurements of total cross sections alone do not provide exhaustive information on the amplitude. An experiment which does make it possible to determine the magnitude and phase of the amplitude for given values of the spin variables in called a "complete experiment." It provides the maximum amount of information about the process and allows the most comprehensive comparison of theory and experiment. In particular, it makes it possible to determine separately the cross sections for direct and exchange scattering. As we have already pointed out, coincidence experiments can be used to determine the magnitudes and relative phase shifts of the amplitudes for the excitation of an atom into various magnetic sublevels of a given level. Experiments with polarized beams provide information on the spin dependence of electron-atom collisions. A coincidence experiment with polarized beams would in principle make it possible to determine the scattering amplitude.[143–145] General questions regarding the theory of polarization effects in electron-atom collisions are discussed in Refs. 146 and 147.

In polarization experiments, a polarized or unpolarized electron beam is scattered by polarized or unpolarized atoms.

Polarized beams of electrons and atoms can be produced in various ways. Different physical processes are utilized here: "chemi-ionization" of optically oriented He atoms in the 2 $^3S$ state, the Fano effect in the scattering of electrons by alkali metal atoms, and the photoionization of polarized atoms, among others (see, e.g., Refs. 148 and 149 and the detailed lists of references there). An extremely popular method today is to make use of photoemission from a GaAs cathode illuminated by circularly polarized laser light.[149] Pierce *et al.*[149] produced an electron beam with a polarization of 43% at a current of 20 $\mu$A with an energy spread $\Delta E = 150$ meV. Experiments have also been carried out in which polarized electrons have been produced through the scattering of a beam of unpolarized electrons by a target of some sort ("double-scattering experiments" [150]). Polarized atoms can be produced by sending an unpolarized atomic beam through a nonuniform magnetic field (a Stern-Gerlach experiment). A technique widely used today is to pump optically a certain sublevel of the hyperfine structure of an atom with circularly polarized laser light.[151] This technique has achieved an 85% polarization of an atomic beam.

There are two types of experiments, differing in the particular quantities which are measured. In the experiments of the first type, one measures either cross sections for processes with given spin states of the particles after scattering or various quantities which characterize the spin states of the electrons and atoms after scattering. In experiments of the second type, one measures the polarization of the photons which are emitted by atoms excited in a collision process.

Among the experiments of the first type are those on the excitation of polarized alkali metal atoms by polarized electrons, which have been carried out by Baum, Schröder, *et al.*[152] They measured the asymmetry $A_{ns\text{-}np}$, defined as

$$A_{ns\text{-}np} = \frac{\sigma(\uparrow\downarrow) - \sigma(\uparrow\uparrow)}{\sigma(\uparrow\downarrow) + \sigma(\uparrow\uparrow)}.$$

Here $\sigma(\uparrow\uparrow)$ and $\sigma(\uparrow\downarrow)$ are the excitation cross sections for the cases in which the spins of the electron and the atom are respectively parallel and antiparallel.

For the parallel spin configuration of the initial state of the particles, the process is described by a triplet cross section $\sigma_T$. For an antiparallel spin configuration, which is a mixture of singlet and triplet states, the cross section is

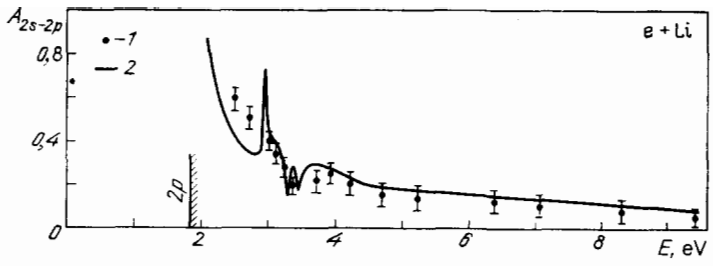


FIG. 24. The asymmetry parameter $A_{2s-2p}$ for e + Li scattering. 1—Experimental[153]; 2—calculations by the diagonalization method.[154]

$$\frac{1}{2}(\sigma_T+\sigma_S).$$

In terms of the singlet and triplet cross sections, the asymmetry can thus be written as

$$A_{ns-np}=\frac{\sigma_S-\sigma_T}{4\sigma},$$

where $\sigma$ is the total cross section given by

$$\sigma = {}^1/_4\sigma_S + {}^3/_4\sigma_T.$$

Figure 24 shows results which have been obtained on the asymmetry parameter $A_{2s-2p}$ for the Li atom. This experiment was carried out by Schröder.[153] Theoretical results have been obtained by the diagonalization method[154] and by the strong coupling method.[155] It can be seen from this figure that the experiments indicate a $^1D$ resonance near the threshold. On the other hand, no resonances associated with excited states of the Li atom have been discovered.

Figure 25 shows the results of a theoretical calculation[98] of the polarization vector of the scattered electrons in the process e + Cs(6s) → e + Cs(6s) for various scattering angles and for various polarization states of the beams. If the beam is incident along the $Z$ axis, and if the scattering plane is the $(x,z)$ plane, the polarization vector $\mathbf{P}$ is perpendicular to this plane, and the nonvanishing component $P_y$ ($|P_y|\leqslant 1$) is equal to the difference between the probabilities ($W_1$ and $W_2$) for electron spin projections $S_y = 1/2$ and $S_y = -1/2$. It can be seen from these figures that $P_y$ is small outside the resonance region, while in the resonance region the curve has a structure which depends strongly on the scattering angle. Unfortunately, we do not yet have any experimental

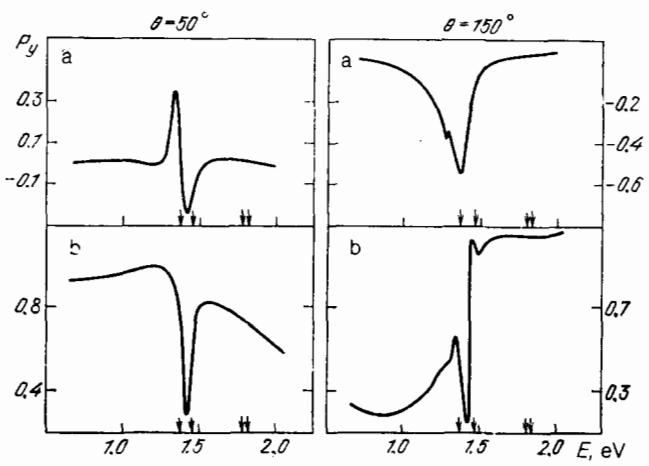


FIG. 25. The polarization vector $P_y$ in e + Cs scattering for various scattering angles and for various polarization states of the beams.[98] a—The electron beam is unpolarized; b—the electron beam is polarized in the transverse direction.

data for comparison with these theoretical results. Such data are available for e + Hg scattering. Albert *et al.*[137] measured the spin polarization of electrons scattered elastically by mercury atoms as a function of the energy over the interval 4–6 eV at several angles. Working from their results, they determined the positions and classification of three resonances: $^2S_{1/2}$ (4.55 eV), $^2D_{3/2}$ (4.71 eV), and $^2D_{5/2}$ (4.49 eV).

Although experiments of the second type, with electrons and atoms unpolarized in their initial state, have been carried out a long time ago, it is only in the last decade that such experiments have been carried out with polarized beams of atoms and electrons. Jitschin *et al.*[157] measured the degree of polarization of the radiation from polarized Na atoms excited by an unpolarized electron beam. No special study was made of resonances in those experiments, however, and there is no evidence of them on the curve of the polarization as a function of the energy of the impinging electrons. An experiment carried out to measure the circular polarization of the radiation emitted after the excitation of the 6s6p $^2P$ level of the mercury atom was used in Ref. 158 to classify resonances.

Although so far there have been relatively few studies of resonances in polarization experiments, the rapid progress which we have seen recently in the apparatus for producing polarized atoms and electrons raises the hope that many interesting new results will be achieved in this direction in the near future.

## 11. CONCLUSION

The material presented above shows that research on resonances in the cross sections for the scattering of electrons by atoms and ions is now an important and urgent problem both theoretically and experimentally. Resonances strongly affect the cross sections for electron scattering by atoms and, to an even greater extent, the cross sections for the scattering of electrons by ions. This influence increases with increasing charge of the ion. As Smirnov has pointed out,[159,160] the presence of autoionizing states of multiply charged ions has a strong effect on the nature of the emission spectrum of a hot plasma. The formation and decay of autoionizing states strongly influence the kinetics of the filling of levels in a low-temperature laser plasma. The role played by autoionizing states in plasmas was studied in detail in Ref. 161.

The number of atoms for which we have a comprehensive picture of the resonances hardly exceeds ten. So far, only the first pages have been written in the spectroscopy of autoionizing states of atoms and ions. Resonance phenomena are a touchstone for testing theoretical models for describing multiparticle interactions. The methods available today,

such as the method of strong coupling of channels, the diagonalization method, and the *R*-matrix method, have been fairly successful in describing resonance effects at low energies. Despite the progress, however, the role played by electron-electron correlations in the formation of autoionizing states has not been studied adequately. As this review has shown, most of the work, both experimental and theoretical, has dealt with collisions of electrons with light atoms. We can apparently expect to see a greater effort on detailed studies of heavy atoms in the future. This problem seems to be completely solvable in view of the significant recent progress in relativistic atomic theory.

Another factor which makes this an important problem is that the topic of resonance phenomena goes beyond the scope of electron-atom collisions, also including resonances in the scattering of electrons by molecules, in atom-atom collisions, in nuclear scattering, and in the scattering of elementary particles. We have not taken up here such interesting and important processes in which resonances are manifested as the recombination of ions, electron-impact ionization, single- and multiphoton ionization of atoms and molecules, and charge exchange of atoms with ions. Each of these topics has been the subject of a formidable list of studies and of special monographs.[162–164]

When the surface of a metal is bombarded with positive ions, negative ions also form on the surface. There is the hope that an expansion of this research will lead to new directions in research on matter.

We might point out yet another research field in which autoionizing states play an important role. Applications in relativistic nuclear physics require research on the ionization of atoms and ions by relativistic electrons.[165] At electron energies of a few MeV, autoionizing states due to the formation of vacancies in inner shells are excited. Theoretically, the problem of the scattering of relativistic electrons requires solution of the relativistic analog of the Schrödinger equation: the Dirac equation. Such calculations have not yet been carried out comprehensively. These processes also pertain to so-called processes with a redistribution of particles. As yet, we do not have an adequate theory for such processes. Much hope here is pinned on an approach based on the use of Faddeev equations.

Since in all these cases we are dealing with a many-body problem, we are attracted to the problem of constructing a unified theory for describing resonances in collisions of composite systems. The field of electron-atom collisions which we have discussed here may serve as a proving ground for testing a unified theory of this sort, since the potential of the interaction between particles is known in this case. This goal can be reached, however, only after more experimental information has been acquired. Here it is very important to obtain more-detailed information on total cross sections in experiments with beams with very small energy spreads and also information embodied in differential cross sections, to carry out phase-shift analyses, and to carry out experiments with polarized beams.


[1]U. Fano, Phys. Rev. **A126**, 1866 (1961).
[2]P. G. Burke and H. M. Shey, Phys. Rev. **A126**, 147 (1962).
[3]M. Gaĭlitis and R. Damburg, Proc. Phys. Soc. **82**, 192 (1963).
[4]G. J. Schulz, Phys. Rev. **A136**, 650 (1964).
[5]C. E. Kuyatt, J. A. Simpson, and S. R. Mielzyarek, Phys. Rev. **A138**, 385 (1965).
[6]A. I. Imre, Ya. N. Semenyuk, and A. I. Dashchenko, Proceedings of the Eighth All-Union Conference on the Physics of Electronic and Atomic Collisions (in Russian), 1981, p. 177.
[7]I. P. Zapesochnyĭ and O. B. Shpenik, Zh. Eksp. Teor. Fiz. **50**, 890 (1966) [Sov. Phys. JETP **23**, 592 (1966)].
[8]H. Hafner, Phys. Lett. **A43**, 275 (1973).
[9]D. Andrick, M. Eyb, and M. Hofmann, J. Phys. **B5**, L15 (1972).
[10]D. Burrow and J. Comer, J. Phys. **B8**, L92 (1975).
[11]N. I. Romanyuk, O. B. Shpenik, and I. P. Zapesochnyĭ, Pis'ma Zh. Eksp. Teor. Fiz. **32**, 472 (1980) [JETP Lett. **32**, 452 (1980)].
[12]O. B. Shpenik, V. V. Sovter, A. N. Zavilopulo, I. P. Zapesochnyĭ, and E. É. Kontrosh, Zh. Eksp. Teor. Fiz. **69**, 48 (1975) [Sov. Phys. JETP **42**, 23 (1975)].
[13]J. N. Bardsley and F. Mandl, Rep. Prog. Phys. **31**, 471 (1968).
[14]P. G. Burke, Adv. Phys. **14**, 521 (1965).
[15]P. G. Burke, Adv. At. Mol. Phys. **4**, 173 (1968).
[16]K. Smith, Rep. Prog. Phys. **29**, 373 (1966).
[17]Y. K. Ho, Phys. Rep. **99**, 1 (1983).
[18]G. J. Schulz, Rev. Mod. Phys. **45**, 378 (1973).
[19]D. E. Golden, Adv. At. Mol. Phys. **14**, 1 (1978).
[20]J. Callaway, Comm. Atom. Mol. Phys. **10**, 279 (1981).
[21]M. K. Gaĭlitis, Usp. Fiz. Nauk **116**, 665 (1975) [Sov. Phys. Usp. **18**, 600 (1975)].
[22]P. G. Burke and M. J. Seaton, Meth. Comput. Phys. **10**, 1 (1971).
[23]M. Gaĭlitis and R. Damburg, Zh. Eksp. Teor. Fiz. **44**, 1644 (1963) [Sov. Phys. JETP **17**, 1107 (1963)].
[24]K. Smith and L. A. Morgan, Phys. Rev. **A165**, 110 (1968).
[25]V. V. Balashov, S. I. Grishanova, I. M. Kruglova, and V. S. Senashenko, Opt. Spektrosk. **28**, 859 (1970) [Opt. Spectrosc. (USSR) **28**, 466 (1970)].
[26]M. I. Gaĭsak V. I. Lend'el, V. T. Navrotskiĭ, and E. P. Sabad, Ukr. Fiz. Zh. **28**, 1798 (1983); **27**, 1617 (1982).
[27]V. I. Lend'el, V. T. Navrotskiĭ, and E. P. Sabad, Ukr. Fiz. Zh. **28**, 1798 (1983); **29**, 1484 (1984).
[28]S. M. Kazakov, V. I. Lend'el, É. A. Masalovich, E.P. Sabad, O. V. Khristoforov, and I. I. Cherlenyak, Ukr. Fiz. Zh. **30**, 502 (1985).
[29]M. I. Gaĭsak, V. I. Lend'el, V. T. Navrotskiĭ, and E. P. Sabad, Preprint ITF-82-13R, Institute of Theoretical Physics, Academy of Sciences of the Ukrainian SSR, Kiev, 1982.
[30]P. G. Burke and W. D. Robb, Adv. At. Mol. Phys. **11**, 143 (1975).
[31]M. J. Seaton, J. Phys. **B15**, 3899 (1982).
[32]M. Ya. Amusia and N. A. Cherepkov, Case Studies Atom. Phys. **5**, 47 (1975).
[33]M. Ya. Amusia and A. S. Kheifets, Phys. Lett. **A82**, 407 (1981).
[34]R. K. Nesbet, Comput. Phys. Commun. **6**, 275 (1973).
[35]M. Ya. Amus'ya and A. S. Kheĭfets, Zh. Eksp. Teor. Fiz. **86**, 1217 (1984) [Sov. Phys. JETP **59**, 710 (1984)].
[36]B. Stumpt and T. F. Gallagher, in: Thirteenth International Conference on the Physics of Electronic and Atomic Collisions, Post-deadline papers, Berlin, 1983, p. 3.
[37]J. P. Ziesel, D. Field, P. M. Guyon, T. R. Govers, M. Lavollee, and O. Dutuint, Thirteenth International Conference on the Physics of Electronic and Atomic Collisions, Berlin, 1983, p. 706.
[38]L. Sanche and G. J. Schulz, Phys. Rev. **A5**, 1672 (1972).
[39]M. Eyb and M. Hofmann, J. Phys. **B8**, 1095 (1975).
[40]V. I. Frontov, A. I. Dashchenko, A. I. Imre, A. N. Gomonaĭ, and I. P. Zapesochnyĭ, Elementary Interaction Processes in Atoms (in Russian), Uzhgor. gos. universitet, Uzhgorod, 1985, p. 16.
[41]O. B. Shpenik, A. N. Zavilopulo, A. V. Snegursky, and I. I. Fabrikant, J. Phys. **B17**, 887 (1984).
[42]V. V. Balashov, S. S. Lipovetsky, and V. S. Senashenko, Phys. Lett. **A38**, 103 (1972).
[43]E. Weigold, in: *Molecular Physics and Quantum Chemistry in '80 Workshop*, Wollongong, February 1980, p. 3.8.1.
[44]R. J. O. Teubner, J. E. Furst, and J. L. Riley, Austr. J. Phys. **35**, 501 (1982).
[45]K. Smith, R. P. McEachran, and P. A. Fraser, Phys. Rev. **A125**, 553 (1962).
[46]P. G. Burke and A. J. Taylor, Proc. Phys. Soc. **88**, 549 (1966).
[47]G. J. Schulz, Phys. Rev. Lett. **13**, 583 (1964).
[48]H. Kleinpoppen and V. Railbe, Phys. Lett. **A18**, 24 (1965).
[49]J. W. McGowan, E. M. Clarke, and E. K. Curley, Phys. Rev. Lett. **15**, 917 (1965).
[50]S. Ormonde, J. McEwen, and J. W. McGowan, Phys. Rev. Lett. **22**, 1165 (1969).
[51]C. D. Warner, G. C. King, P. Hammond, and J. Slevin, Fourteenth International Conference on the Physics of Electronic and Atomic Collisions, Palo Alto, 1985, p. 142.
[52]J. F. Williams, J. Phys. **B9**, 1519 (1976).
[53]J. Callaway, Phys. Rev. **A26**, 199 (1982).
[54]L. C. G. Freitas, K. A. Berrington, P. G. Burke, A. Hibbert, A. E.

Kingston, and A. L. Sinfailam, J. Phys. **B7**, L303 (1984).
[55]D. E. Golden, F. D. Schowengerdt, and J. Macek, J. Phys. **B7**, 478 (1974).
[56]D. Andrick and L. Langhas, J. Phys. **B8**, 1245 (1975).
[57]D. W. O. Heddle, Proc. R. Soc. London **A352**, 441 (1977).
[58]R. G. W. Kessing, Proc. R. Soc. London **A352**, 429 (1977).
[59]D. Spence, D. Stuit, M. A. Dillon, and R. G. Wang, in: Thirteenth International Conference on the Physics of Electronic and Atomic Collisions, Berlin, 1983, p. 117.
[60]D. W. O. Heddle, R. G. W. Keesing, and J. M. Kurepa, Proc. R. Soc. London **A334**, 135 (1973).
[61]H. S. W. Massey, *Negative Ions*, Cambridge Univ. Press, 1976 (Russ. transl., Mir, M., 1979).
[62]H. W. Dassen *et al.*, Eleventh International Conference on the Physics of Electronic and Atomic Collisions, Gatlinburg, 1981, p. 196.
[63]D. Spence, J. Phys. Ser. **B14**, 129 (1981).
[64]H. W. Dassen, R. Gomes *et al.*, J. Phys. Ser. **B16**, 1481 (1983).
[65]F. H. Read, Phys. Script. **27**, 103 (1983).
[66]N. S. Scott, K. L. Bell, P. G. Burke, and K. T. Taylor, J. Phys. **B15**, L627 (1982).
[67]D. F. Dance, W. F. A. Harrison, and A. C. H. Smith, Proc. R. Soc. London **A290**, 73 (1966).
[68]B. Peart and K. T. Dolder, J. Phys. **B6**, 2415 (1973).
[69]S. Ormonde, W. Whitaker, and L. Lipsky, Phys. Rev. Lett. **19**, 1161 (1967).
[70]A. I. Dashchenko, A. I. Imre, and I. P. Zapesochnyĭ, Pis'ma Zh. Eksp. Teor. Fiz. **19**, 223 (1974) [JETP Lett. **19**, 137 (1974)].
[71]A. I. Dashchenko, I. P. Zapesochnyĭ, A. I. Imre, V. S. Vukstich, F. F. Danch, and V. A. Kel'man, Zh. Eksp. Teor. Fiz. **67**, 503 (1974) [Sov. Phys. JETP **40**, 249 (1975)].
[72]Ya. N. Semenyuk, Ukr. Fiz. Zh. **29**, 1252 (1984).
[73]P. G. Burke and A. J. Taylor, J. Phys. **B2**, 44 (1969).
[74]S. Wakid and J. Callaway, Phys. Lett. **A78**, 137 (1980).
[75]N. R. Daly and R. E. Powell, Phys. Rev. Lett. **19**, 1165 (1967).
[76]R. J. W. Henry, Phys. Rep. **68**, 1 (1981).
[77]É. M. Karule, Effective cross sections for electron-atom collisions (in Russian), Zinatne, Riga, 1965, No. 3, p. 33.
[78]A. L. Sinfailam and R. K. Nesbet, Phys. Rev. **A7**, 1987 (1973).
[79]V. R. Kaulakis, Opt. Spektrosk. **48**, 574 (1980) [Opt. Spectrosc. (USSR) **48**, 315 (1980)].
[80]I. I. Fabrikant, Opt. Spektrosk. **53**, 223 (1982) [Opt. Spectrosc. (USSR) **53**, 131 (1982)].
[81]A. R. Jonston and P. D. Burrow, J. Phys. **B15**, L745 (1982).
[82]H. T. Saelee and J. Lukas, J. Phys. **D12**, 1257 (1979).
[83]L. M. Biberman, A. Kh. Mnatsakanyan, and I. T. Yakubob, Usp. Fiz. Nauk **102**, 431 (1970) [Sov. Phys. Usp. **13**, 728 (1970)].
[84]P. G. Burke and A. J. Taylor, J. Phys. **B2**, 859 (1969).
[85]A. C. Fung and J. J. Matese, Phys. Rev. **A5**, 22 (1972).
[86]C. D. Lin, J. Phys. **B16**, 726 (1983).
[87]B. Jadusliver, A. Tino, and B. Bederson, Phys. Rev. **A24**, 1249 (1981).
[88]V. I. Lend'el, E. P. Sabad, and I. I. Cherlenyak, Elementary processes in atomic collisions (in Russian), Cheboksary, 1984, p. 21.
[89]J. Perel, P. Englander, and B. Bederson, Phys. Rev. **A128**, 1148 (1962).
[90]S. M. Kazakov and O. V. Khristoforov, Fourteenth International Conference on the Physics of Electronic and Atomic Collisions, Post-deadline papers, Palo Alto, 1985, p. 144.
[91]V. V. Ignatishin and I. I. Cherlenyak, in: Elementary Interaction Processes in Atoms (in Russian), Uzhgor. gos. universitet, Uzhgorod, 1985, p. 53.
[92]D. L. Moores, J. Phys. **B9**, 1329 (1976).
[93]C. H. Greene, Phys. Rev. **A23**, 661 (1981).
[94]M. Eyb, J. Phys. **B9**, 101 (1976).
[95]P. G. Burke and J. F. Mitchel, J. Phys. **B7**, 215 (1974).
[96]W. Gehen and E. Reichert, J. Phys. **B10**, 3105 (1977).
[97]N. S. Scott, K. Bartschat, P. G. Burke, and W. B. Eissner, J. Phys. **B17**, L195 (1984).
[98]N. S. Scott, K. Bartschat, P. G. Burke, O. Nogy, and W. B. Eissner, J. Phys. **B17**, 3755 (1984).
[99]F. H. Read, Austr. Phys. **35**, 475 (1982).
[100]U. Fano, Rep. Prog. Phys. **46**, 97 (1983).
[101]C. D. Lin, Phys. Rev. **A32**, 760 (1974).
[102]S. I. Nikitin and V. N. Ostrovskiĭ, Physics of Molecules (in Russian), ITF Akad. Nauk Ukr. SSR, Kiev, 1980, No. 3, p. 3.
[103]V.P. Zhigutov and B. N. Zakhar'ev, Methods of strong channel coupling in quantum scattering theory (in Russian), Atomizdat, M., 1974.
[104]Yu. F. Smirnov and K. V. Shitikova, Fiz. Elem. Chastits At. Yadra **8**, 344 (1977) [*sic*].
[105]I. H. Macek. J. Phys. **B1**, 851 (1968).
[106]R. G. Athay, Astrophys. J. **146**, 223 (1966).
[107]M. I. Gaĭsak, V. I. Lend'el, and V. Yu Poĭda, Perturbation Theory in Atomic Calculations (in Russian), Sovet po spektroskopii Akad. Nauk SSSR, Moscow, 1985, p. 128.
[108]M. I. Gaĭsak, V. I. Lend'el, and V. Yu Poĭda, Abstracts of Papers Presented at the Seventh All-Union Conference on the Physics of Vacuum-UV Radiation and its Interaction with Matter (in Russian), Latv. gos. universitet, Ézernieki, 1986, p. 129.
[109]M. I. Gaĭsak, V. I. Lend'el, and V. Yu. Poĭda, in: Abstracts of Papers Presented at the Ninth All-Union Conference on the Theory of Atoms and Atomic Spectra (in Russian), Uzhgorod, 1985, p. 61.
[110]G. G. Petrash, Usp. Fiz. Nauk **105**, 645 (1971) [Sov. Phys. Usp. **14**, 747 (1972)].
[111]V. V. Zhukov, V. S. Kucherov, E. L. Latush, and M. F. Sém, Kvant Elektron. (Moscow) **4**, 1257 (1977) [Sov. J. Quantum Electron. **7**, 708 (1977)].
[112]L. P. Presnyakov and A. M.Urnov, Zh. Eksp. Teor. Fiz. **68**, 61 (1975) [Sov. Phys. JETP **41**, 31 (1975)].
[113]V. A. Bazylev and M. I. Chibisov, Usp. Fiz. Nauk **133**, 617 (1981) [Sov. Phys. Usp. **24**, 276 (1981)].
[114]I. P. Zapesochnyĭ, A. I. Dashchenko, V. I. Frontov, A. I. Imre, A.N. Gomonaĭ, V. I. Lend'el, V. T. Navrotskiĭ, and E. P. Sabad, Pis'ma Zh. Eksp. Teor. Fiz. **39**, 45 (1984) [JETP Lett. **39**, 51 (1984)].
[115]V. I. Frontov, A. I. Dashchenko, A. I. Imre, and I. P. Zapesochnyĭ, in: Abstracts of Papers Presented at the Ninth All-Union Conference on the Physics of Electronic and Atomic Collisions (in Russian), Riga, 1984, p. 33.
[116]P. D. Taylor, R. A. Phaneuf, and G. H. Dunn, Phys. Rev. **A22**, 435 (1980).
[117]V. I. Lend'el, É. A. Masalovich, V. T. Navrotskiĭ, and E. P. Sabad, Izv. Vyssh. Uchebn. Zaved., Fiz. No. 2, 110 (1985).
[118]M. A. Hayes, D. W. Norcross, J. B. Mann, and D. W. Robb, J. Phys. **B10**, L429 (1977).
[119]V. A. Kel'man, A. I. Dashchenko, I. P. Zapesochnyĭ, and A. P. Imre, Dokl. Akad. Nauk SSSR **220**, 65 (1975) [Sov. Phys. Dokl. **20**, 38 (1975)].
[120]V. I. Frontov, Opt. Spektrosk. **59**, 460 (1985) [Opt. Spectrosc. (USSR) **59**, 277 (1985)].
[121]V. I. Frontov, A. I. Dashchenko, A. I. Imre, and I. P. Zapesochnyĭ, Ukr. Fiz. Zh. **30**, 833 (1985).
[122]C. Mendoza, J. Phys. **B14**, 2465 (1981).
[123]P. G. Burke and D. L. Moores, J. Phys. **B1**, 575 (1968).
[124]A. I. Zapesochnyĭ, A. I. Imre, I. S. Aleksakhin, I. P. Zapesochnyĭ, and O. I. Zatsarinnyĭ, Zh. Eksp. Teor. Fiz. **90**, 1972 (1986) [Sov. Phys. JETP **63**, 1155 (1986)].
[125]I. P. Zapesochnyĭ, A. I. Imre, E. É. Kontrosh, I. P. Zapesochnyĭ, and A. N. Gomonaĭ, Pis'ma Zh. Eksp. Teor. Fiz. **43**, 463 (1986) [JETP Lett. **43**, 596 (1986)].
[126]F. D. Burrow, J. A. Micheida, and J. Comer, J. Phys. **B9**, 3225 (1976).
[127]O. B. Shpenik, I. P. Zapesochnyĭ, V. V. Sovter, E. I. Nepijpov *et al.*, Tenth International Conference on the Physics of Electronic and Atomic Collisions, Paris, 1977, p. 1302.
[128]O. B. Shpenik, I. P. Zapesochnyĭ, E. É. Kontrosh, É. I. Nepiĭpov, N. I. Romanyuk, and V. V. Sovter, Zh. Eksp. Teor. Fiz. **76**, 846 (1979) [Sov. Phys. JETP **49**, 426 (1979)].
[129]H. A. Kurtz and Y. Ohrn, Phys. Rev. **A19**, 43 (1979).
[130]I. I. Fabrikant, Atomic Processes (in Russian), Zinatne, Riga, 1975, p. 80.
[131]M. Ya. Amus'ya, V. A. Sosnivker, N. A. Cherepkov, and L. V. Chernysheva, Preprint No. 863, Physicotechnical Institute, Academy of Sciences of the USSR, L., 1983.
[132]N. I. Romanyuk, Author's Abstract, Candidate's Dissertation (in Russian), Uzhgorod, 1981.
[133]I. P. Zapesochnyĭ and O. B. Shpenik, Dokl. Akad. Nauk SSSR **160**, 1053 (1965) [Sov. Phys. Dokl. **10**, 140 (1965)].
[134]U. Fano and J. W. Cooper, Phys. Rev. **A138**, 400 (1965).
[135]T. W. Ottley and H. Kleinpoppen, J. Phys. **B8**, 400 (1975).
[136]D. S. Newman, G. C. King, and M. Zubek, in: Thirteenth International Conference on the Physics of Electronic and Atomic Collisions, Berlin, 1983, p. 104.
[137]K. Albert, C. Christian, T. Heindorff, E. Reichert, and S. Schön, J. Phys. **B10**, 3733 (1977).
[138]D. W. O. Heddle, J. Phys. **B11**, L711 (1978).
[139]S. M. Kazakov, A. I. Korotkov, and O. B. Shpenik, Zh. Eksp. Teor. Fiz. **78**, 1687 (1980) [Sov. Phys. JETP **51**, 847 (1980)].
[140]N. S. Scott, P. G. Burke, and K. Bartschat, in: Thirteenth International Conference on the Physics of Electronic and Atomic Collisions, Berlin, 1983, p. 103.
[141]I. S. Aleksakhin, S. B. Zagrebin, I. P. Zapesochnyĭ, D. A. Ozolin'sh, A. V. Samson, and I. I. Shafran'osh, in: Excitation and Ionization Photoprocesses: Proceedings of a Soviet-Yugoslav Seminar (in Russian), L., 1984, p. 74.
[142]I. I. Shafran'osh, T. A. Snegurskaya, and I. S. Aleksakhin, Thirteenth International Conference on the Physics of Electronic and Atomic

Collisions, Berlin, 1983, p. 98.
[143]G. F. Hanne, in: Coherence and Correlation in Atomic Physics (H. Kleinpoppen and J. Williams, editors), New York, 1980.
[144]S. M. Khalid and H. Kleinpoppen, J. Phys. **B17**, 243 (1984).
[145]T. T. Gien, J. Phys. **B15**, 4617 (1982).
[146]G. F. Drukarev and V. D. Ob'edkov, Usp. Fiz. Nauk **127**, 621 (1979) [Sov. Phys. Usp. **22**, 236 (1979)].
[147]J. Kessler, *Polarized Electrons*, Springer-Verlag, New York, 1976.
[148]B. N. Delone and M. V. Fedorov, Usp. Fiz. Nauk **127**, 651 (1979) [Sov. Phys. Usp. **22**, 252 (1979)].
[149]D. T. Pierce *et al.*, Rev. Sci. Instrum. **51**, 478 (1980).
[150]G. F. Hanne and J. Kessler, J. Phys. **B9**, 791 (1976).
[151]D. Hils, W.Litschin, and H. Kleinpoppen, Appl. Phys. **25**, 39 (1981).
[152]G. Baum, E. Kisker, W. Raith, W. Schröder, U. Sillmen, and D. Zenses, J. Phys. **B14**, 4377 (1981).
[153]W. Schröder, Ph.D. Thesis, Universitat Bielefeld, 1982.
[154]V. I. Lend'el, M. M. Molnar, E. P. Sabad, and I. I. Cherlenyak, in: Abstracts of Papers Presented at the Ninth All-Union Conference on the Physics of Electron and Atomic Collisions), Riga, 1984, p. 36.
[155]G. Baum, M. Moede, W. Raith, and U. Sillmen, in: Fourteenth International Conference on the Physics of Electronic and Atomic Collisions, Palo Alto, 1985, p. 182.
[156]D. D. Oza, Phys. Rev. **A33**, 824 (1986).
[157]W. Jitschin, S. Osimitsh, H. Reihe, and H. Kleinpoppen, in: Thirteenth International Conference on the Physics of Electronic and Atomic Collisions, Berlin, 1983, p. 150.
[158]A. Wolcke, K. Bartschat *et al.*, J. Phys. **B16**, 639 (1983).
[159]B. M. Smirnov, Atomic Collisions and Elementary Processes in Plasmas (in Russian), Atomizdat, M., 1968.
[160]B. M. Smirnov, Excited Atoms (in Russian), Energoatomizdat, Moscow, 1982.
[161]E. V. Aglitskiĭ and U. I. Safronova, Spectroscopy of Autoionization States of Atomic Systems (in Russian), Énergoatomizdat, M., 1985.
[162]N. B. Delone and V. P. Kraĭnov, An Atom in an Intense Optical Field (in Russian), Énergoatomizdat, M., 1984.
[163]L. A. Vaĭnshteĭn, I. I. Sobel'man, and E. A. Yukov, Excitation of Atoms and Spectral Line Broadening (in Russian), Nauka, M., 1979.
[164]V. M. Galitskiĭ, E. E. Nikitin, and B. M. Smirnov, Theory of Collisions of Atomic Particles (in Russian), Nauka, M., 1981.
[165]E. A. Perelstein and G. D. Shirkov, Preprint JINR E9-85-4, Dubna, 1985.
[166]K. A. Berrington, P. G. Burke, and A. L. Sinfailam, J. Phys. **B8**, 1459 (1975).
[167]B. F. Davis and K. T. Chung, Phys. Rev. **A29**, 1878 (1984).
[168]R. E. Kennerly, R. J. van Brunt, and A. C. Gallagher, Phys. Rev. **A23**, 2430 (1981).
[169]D. E. Golden and A. Zecca, J. Phys. **A1**, 241 (1970).
[170]F. M. J. Pichanick and J. A. Simpson, Phys. Rev. **A168**, 64 (1968).
[171]H. Ehrhardt, L. Langhans, F. Linder, and H. S. Taylor, Phys. Rev. **A173**, 222 (1968).
[172]M. Blaha, Astron. Astrophys. **16**, 437 (1972).
[173]R. S. Oberoi and R. K. Nesbet, Phys. Rev. **A8**, 2969 (1973).
[174]S. Cvejanovic, J. Comer, and F. H. Read, J. Phys. **B7**, 468 (1974).
[175]P. G . Burke, L. C. G. Freitas, A. E. Kingston, and K. A. Berrington, Thirteenth International Conference on the Physics of Electronic and Atomic Collisions, Berlin, 1983, p. 108.

Translated by Dave Parsons